Quaternary Science Reviews 242 (2020) 106468

Contents lists available at ScienceDirect

Quaternary Science Reviews

journal homepage: www.elsevier.com/locate/quascirev

The Holocene *Cedrus* pollen record from Sierra Nevada (S Spain), a proxy for climate change in N Africa

Gonzalo Jiménez-Moreno [a, *], R. Scott Anderson [b], María J. Ramos-Román [a, c], Jon Camuera [a, c], Jose Manuel Mesa-Fernández [a, d], Antonio García-Alix [a, d], Francisco J. Jiménez-Espejo [d], José S. Carrión [e], Alejandro López-Avilés [a]

[a] Departamento de Estratigrafía y Paleontología, Universidad de Granada, Spain
[b] School of Earth and Sustainability, Northern Arizona University, USA
[c] Department of Geosciences and Geography, University of Helsinki, Helsinki, Finland
[d] Instituto Andaluz de Ciencias de la Tierra (IACT), CSIC-UGR, Armilla, Spain
[e] Department of Plant Biology, Faculty of Biology, University of Murcia, Spain

ARTICLE INFO

Article history:
Received 16 April 2020
Received in revised form
30 June 2020
Accepted 30 June 2020
Available online 21 July 2020

Keywords:
Cedrus
Holocene
Climate
Sierra Nevada
Western mediterranean
Windblown pollen

ABSTRACT

Comprehending the effects of climate variability and disturbance on forested ecosystems is paramount to successfully managing forest environments under future climate scenarios (e.g., global warming, aridification increase). Changes in fossil pollen abundance in sedimentary archives record past vegetation dynamics at regional scales, mainly related to climate changes and, in the last few millennia, to human impact. Pollen records can thus provide long databases with information on how the environment reacted to climate change before the historical record. In this study, we synthesized fossil pollen data from seven sites from the Sierra Nevada in southern Spain to investigate the response of forests in the western Mediterranean area to millennial-scale climate changes and to human impact during the Holocene. In particular, here we focused on *Cedrus* pollen abundances, which most-likely originated from Northern Africa and were carried to Sierra Nevada by wind. *Cedrus* pollen has received little attention in the Iberian Peninsula palynological records, for it occurs in low concentrations and has an African source, and thus this article explores the potential to reconstruct its past history and climate. Although *Cedrus* abundances are generally lower than 1% in the studied pollen samples, a comparison with North African (Moroccan) *Cedrus* pollen records shows similar trends at long- and short-term time-scales. Therefore, this record could be used as a proxy for changes in this forest species in North Africa. As observed in the Sierra Nevada synthetic record, the increasing trend of *Cedrus* pollen during the Middle and Late Holocene closely correlates with decreasing summer insolation. This would have produced overall cooler annual temperatures in Northern Africa (Middle Atlas and Rif Mountains) as well as lower summer evaporation, benefiting the growth of this cool-adapted montane tree species while increasing available moisture during the summer, which is critical for this water-demanding species. Millennial-scale variability also characterizes the Sierra Nevada *Cedrus* synthetic pollen record. *Cedrus* abundance oscillations co-vary with well-known millennial-scale climatic variability that controlled cedar abundance and altitudinal distribution in montane areas of N Africa.

1. Introduction

Mountain and alpine environments are especially fragile and sensitive to climate change (Thuiller et al., 2005). The stress of recent climate warming is causing altitudinal displacements of forest species and other organisms towards higher latitudes or higher elevation cooler and moister areas (Gehrig-Fasel et al., 2008; Malanson et al., 2019). Previous studies also show that the increase in drought conditions in the Mediterranean area is inducing tree mortality of humidity sensitive forest species such as *Cedrus atlantica* in the Middle Atlas and Rif mountains of Morocco (Cheddadi et al., 2009; Linares et al., 2011). The present-day situation of *Cedrus atlantica* in those two areas is worrisome as

* Corresponding author.
E-mail address: gonzaloj@ugr.es (G. Jiménez-Moreno).

https://doi.org/10.1016/j.quascirev.2020.106468
0277-3791/

indicated by several recent studies (Abel-Schaad et al., 2018; Copes-Gerbitz et al., 2019). The loss in mountain biodiversity could be seriously intensified if drought and forest fires are enhanced in the Mediterranean area, which is forecasted for the next decades (Sánchez et al., 2004; IPPC, 2013). Climatic predictions are important in efforts to reduce the impact of climate change on vulnerable protected mountain environments and climatically sensitive species. Similarly, the study of past climate changes can be used to improve our understanding of future climate scenarios by providing information on how mountain environments reacted to long-term and millennial-to-centennial variations in climate during the Holocene, especially during warmer and drier climate conditions.

A significant effort has recently been made in this regard in the western Mediterranean with the palynological study of the Holocene sedimentary records from several alpine and montane wetlands in southern Spain (Carrión et al., 2003, 2007; Anderson et al., 2011; Jiménez-Moreno and Anderson, 2012; Jiménez-Moreno et al., 2013; Ramos-Román et al., 2016, 2018a; 2018b; Mesa-Fernández et al., 2018; Camuera et al., 2018, 2019; Manzano et al., 2019), montane wetland records from northern Morocco (Lamb and van der Kaars, 1995; Lamb et al., 1999; Cheddadi et al., 2009, 2017; Nour et Bait et al., 2014; Campbell et al., 2017) and marine records from the Alboran Sea (Fletcher and Sanchez Goñi, 2008; Combourieu Nebout et al., 2009). Fossil pollen of *Cedrus* has been recorded in the above-mentioned studies and many other Holocene records from Europe (see syntheses in Magri and Parra, 2002; Magri, 2012; Magri et al., 2017; Alba-Sánchez et al., 2018). However, the European record of *Cedrus* has been difficult to interpret mostly due to its sporadic occurrence, usually lower than 1%, in most pollen records. This is because *Cedrus* pollen is characterized by short distance dispersal and fails to be well distributed in the environment far from the source trees (e.g., Bell and Fletcher, 2016). Some authors suggest that *Cedrus* could have persisted in refuge areas in S Europe in Holocene times (González-Sampériz et al., 2010; Postigo-Mijarra et al., 2010), while others explain those occurrences as due to long-distance transport from N Africa (Magri and Parra, 2002), claiming for instance, that the Holocene *Cedrus* occurrences are connected with increased eolian activity during dry spells such as the 8.2 and 4.2 ka events. The high number of pollen records obtained from the Sierra Nevada area (Fig. 1) allows us, for the first time, to conduct a detailed study and comparison of *Cedrus* occurrence at a regional scale, compensating the limitation of the single site per region approach.

Cedrus is an endemic conifer tree living today at mid elevations (above ~1500 and up to ~2500 m.a.s.l.) on mountains around the Mediterranean in northern Africa (Rif and Atlas Mountains) and the Middle East (Turkey, Syria, Lebanon) (Quézel and Médail, 2003). This taxon is well adapted for cool to cold climatic conditions and it is best represented in humid to subhumid climates (Quézel and Médail, 2003; Cheddadi et al., 2017). *Cedrus* decreased its distribution and subsequently disappeared from the northern Mediterranean area due to the drying and cooling trend that occurred globally in the Neogene and Pleistocene (Zachos et al., 2001; Jiménez-Moreno et al., 2010; Magri, 2012). In the western Mediterranean area, its occurrence is at present restricted to mountain areas of northern Morocco, Algeria and Tunisia. The cedar wood is much appreciated for its durability and has been an important timber in the Mediterranean area, probably being exploited in the last two millennia (Lamb and van der Kaars, 1995). At present, *Cedrus atlantica* is considered an endangered species, for its populations keep declining due to human activities including pastoralism and wood harvesting, climate change and fires (Quézel and Médail, 2003; Cheddadi et al., 2017).

Understanding the Holocene pollen record of *Cedrus* from Europe in relation to that of N Africa, will help us understand the Holocene biogeography of the species, as well as any variations in air masses blowing from Africa (Magri and Parra, 2002). In this study we synthetized Holocene *Cedrus* pollen data from seven alpine and mountain wetland sites from the Sierra Nevada. The study sites are located within 10 km of each other and are subjected to a similar geographic-climatic setting (Table 1). These pollen records of *Cedrus* show an increasing trend in abundance in the Middle and Late Holocene, and depict short-term variability at millennial- and centennial-scales. In order to find shared patterns, minimize the local differences between the records and the potential error of individual site chronologies we synthetized the *Cedrus* pollen data from the Sierra Nevada into a single plot. In addition, we synthesized *Cedrus* pollen data from N Africa, the main source area of the pollen transported to Sierra Nevada, to make a comparison between records and gain insight about the significance of *Cedrus* in European pollen records.

1.1. Geographic setting

Sierra Nevada is a west-east mountain range located in southeastern Spain featuring the tallest peaks in the Iberian Peninsula (23 peaks above 3000 m asl, including Mulhacén: 3479 m asl; Fig. 1A). Climate in the Sierra Nevada area is Mediterranean, with mild winters and hot and dry summers, and is characterized by mean annual temperatures ranging between ~15.5 and 2.5 °C between 725 and 3097 m asl, and annual precipitation between ~418 and ~750 mm between 725 and 2500 m asl (Pérez-Luque et al., 2012; García-Alix et al., 2018; Agencia Estatal de Meteorología AEMET, 2020).

The Rif and Atlas Mountains are the main and highest mountain ranges in northern Morocco and northern Africa, with highest peaks of 2456 and 4167 m, respectively. The Rif Mountains are characterized by receiving the highest precipitation than any other area in Morocco, generally between ~500 and 900 mm with certain areas above 2000 mm/year (Cheddadi et al., 2017). *Cedrus atlantica* and other conifers occur forming forests in those high-elevation humid areas (Cheddadi et al., 2017). Climate in northern Morocco is also Mediterranean, with warm and dry summers and mild and humid fall and winter (Trigo et al., 2002).

The western Mediterranean area is also influenced by the North Atlantic Oscillation (NAO), an atmospheric phenomenon controlling winter climate variability in the North Atlantic and neighboring areas. The NAO controls the intensity and location of the westerlies and therefore winter precipitation in the study area (Trigo et al., 2004). In summertime, the western Mediterranean is subjected to the expansion of the Azores High towards a northeasterly position producing warm-dry summers (Trigo et al., 2004; Lionello et al., 2006). The main wind directions in Sierra Nevada are westerly during winter, with southerly and southwesterly winds happening during spring, summer and fall associated with the weakening of the westerlies (see wind direction for the Granada area in Fig. 1B; https://www.woeurope.eu; Fig. 2).

2. Material and methods

In this study we used *Cedrus* data from seven well-dated Holocene pollen records from wetland sites located at different elevation and orientations in the Sierra Nevada area (Fig. 1D; Table 1). These sedimentary lake and bog archives were recovered by many of the authors between 2006 and 2015 (Table 1). Six of the studied sites are situated above treeline in the cryoromediterranean vegetation belt where typical vegetation is alpine tundra, while one site occurs in the mesomediterranean vegetation belt, where natural vegetation is mostly characterized by evergreen sclerophyllous oak

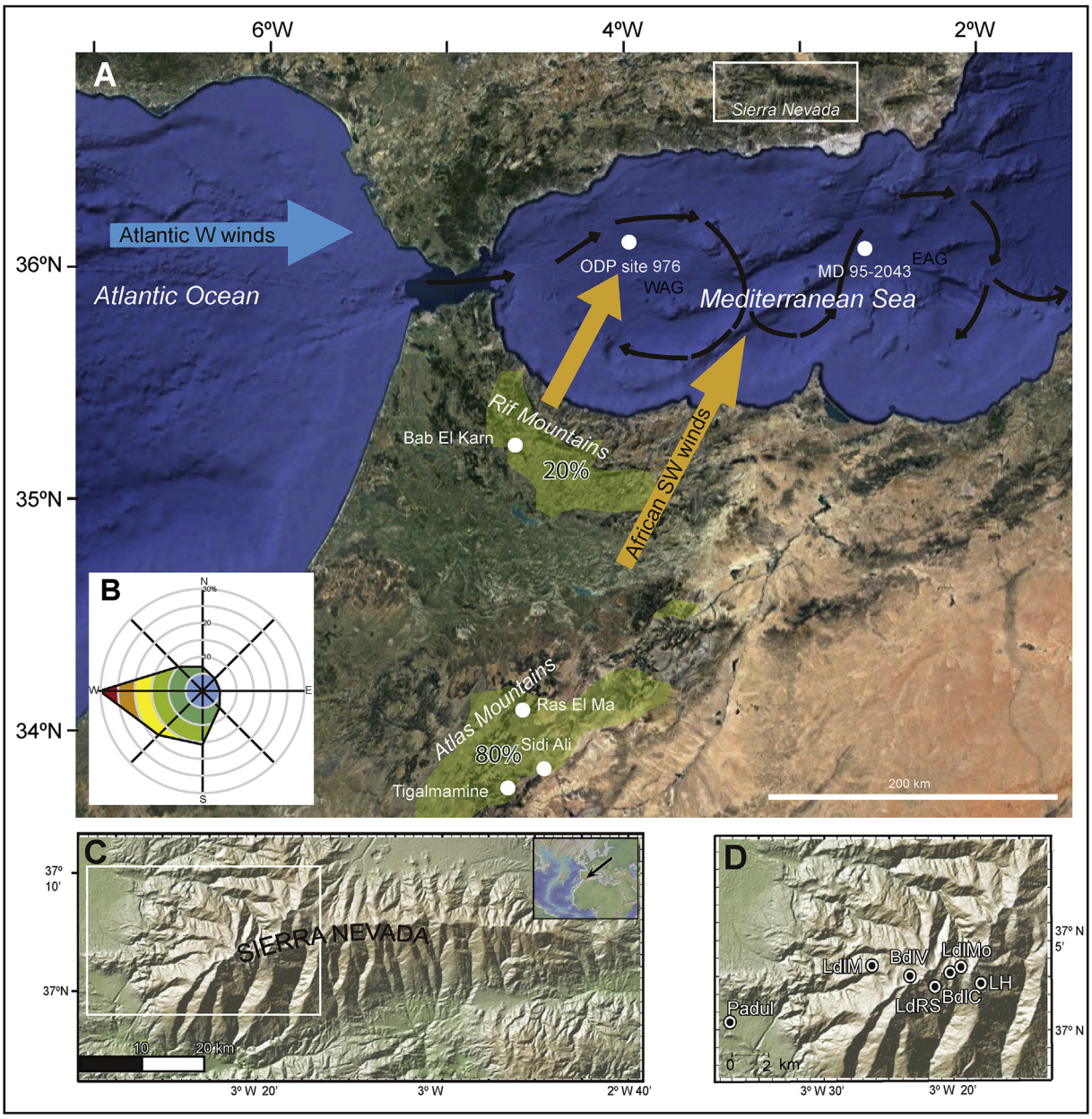

Fig. 1. Location of western Mediterranean Holocene *Cedrus* sites used in this analysis. (A) Map of NW Africa and S Iberia showing the location of sites in the Middle Atlas, Rif, Sierra Nevada mountain and Alboran Sea areas. See text for explanation. (A) schematic natural distribution of *Cedrus atlantica* at present is represented in green shading (from Quézel and Médail, 2003). Note that 80% of *Cedrus* in Morocco is distributed in the Atlas region at present (Linares et al., 2011; Cheddadi et al., 2017). The remaining 20% occurs in the Rif Mountains. Yellow and blue arrows represent main SW and W winds affecting the study area. Black arrows trace the general marine surface circulation (Ausín et al., 2015). WAG: Western Anticyclonic Gyre. EAG: Eastern Anticyclonic Gyre. (B) Wind direction in percentage from January 2000 to December 2019 for Granada, Spain (data obtained from https://www.woeurope.eu); (C) Magnification of Sierra Nevada geographic area; (D) Location of Sierra Nevada *Cedrus* pollen records used in this study: Laguna de Río Seco (LdRS; Anderson et al., 2011), Borreguil de la Caldera (BdlC; Ramos-Román et al., 2016), Borreguil de la Virgen (BdlV; Jiménez-Moreno and Anderson, 2012); Laguna de la Mosca (LdlMo; Manzano et al., 2019), Laguna Hondera (LH; Mesa-Fernández et al., 2018), Laguna de la Mula (LdlM; Jiménez-Moreno et al., 2013), and Padul-15-05 (Padul; Ramos-Román et al., 2018a,b). (For interpretation of the references to color in this figure legend, the reader is referred to the Web version of this article.)

forests. Three sites – Laguna de la Mula (LdlM) (Jiménez-Moreno et al., 2013), Laguna de la Mosca (LdlMo) (Manzano et al., 2019) and Borreguil de la Virgen (BdlV) (Jiménez-Moreno and Anderson, 2012) – are situated at the north-facing side of the Sierra Nevada, while three others – Laguna de Río Seco (LdRS) (Anderson et al., 2011), Borreguil de la Caldera (BdlC) (Ramos-Román et al., 2016) and Laguna Hondera (LH) (Mesa-Fernández et al., 2018) – are located in the south face. The Padul wetland site is located at the southwest foothills of the Sierra Nevada (Ramos-Román et al., 2018a, 2018b). These sites are thus situated between ~725 m asl in the mesomediterranean to ~3020 m asl in the cryoromediterranean vegetation belt (Table 1).

We also used Holocene *Cedrus* pollen data from wetland sites from N Morocco from the Middle Atlas: Sidi Ali (Lamb et al., 1995; Campbell et al., 2017), Tigalmamine (Lamb and van der Kaars, 1995), Ras El Ma (Nour el Bait et al., 2014), Rif Mountains: Bab El Karn (Cheddadi et al., 2016, 2017); and the Mediterranean (Alboran) Sea: ODP site 976 (Combourieu Nebout et al., 2009) and MD 95-2043 (Fletcher and Sanchez Goñi, 2008) for comparison with the synthetic pollen record from Sierra Nevada (Table 1).

Sierra Nevada *Cedrus* stack for the last 11,000 cal yr BP was obtained using seven detailed (resolution between 57 and 232-yrs)

Table 1
Site description of the Sierra Nevada, Morocco and Alboran Sea *Cedrus* records used in this study. Sites from the Sierra Nevada are: BdlV = Borreguil de la Virgen; LdlMo = Laguna de la Mosca; LdlM = Laguna de la Mula; LdRS = Laguna de Río Seco; BdlC = Borreguil de la Caldera; LH = Laguna Hondera; Padul = Padul peat bog. Asterisks (*) indicate information for the Holocene part of those sedimentary records.

	Coordinates and altitude (m asl)	Vegetation belt	Site environment	Core length (cm)	Period covered (cal yr BP)	Dating method	Reference
BdlV	37°03′15"N, 3° 22′40″ W; 2945 m	Cryoromediterranean	Wetland/ peatland	169	0–8200	9 ^{14}C dates	Jiménez-Moreno and Anderson, (2012)
LdlMo	37°03′34.88"N, 3°18′52.98"W; 2889 m	Cryoromediterranean	Lake	190	0–8300	10 ^{14}C dates	Manzano et al. (2019)
LdlM	37°3.583′N, 3°25.017′W; 2497 m	Cryoromediterranean	Lake	32.5	0–4000	6 ^{14}C dates	Jiménez-Moreno et al. (2013)
LdRS	37°02.43"N, 3°20.57′W; 3020 m	Cryoromediterranean	Lake	150	0–11000	9 ^{14}C dates, 1 ^{137}Cs, 1 ^{210}Pb	Anderson et al. (2011)
BdlC	37°03′02" N, 3°19′24" W; 2992 m	Cryoromediterranean	Wetland/ peatland	56	0–4400	5 ^{14}C dates	Ramos-Román et al. (2016)
LH	37°02.88′N, 3°17.66′W; 2899 m	Cryoromediterranean	Lake	83	0–9500	7 ^{14}C dates	Mesa-Fernández et al. (2018)
Padul	37°00′39.77"N, 3°36′14.06"W; 725 m	Mesomediterranean	Wetland/ peatland	327*	0–11000	14 ^{14}C dates*	(Ramos-Román et al., 2018; Ramos-Román et al., 2018b)
Sidi Ali	33° 03′N, 05° 00′ W; 2080 m	Oromediterranean	Lake	1956	0–11000	26 ^{14}C dates, 1, ^{210}Pb/137Cs	Campbell et al. (2017)
Tigalmamine	32°54′ N 05°21′ W; 1626 m	Supramediterranean	Lake	1600	0–11000	11 ^{14}C dates	Lamb and van der Kaars, (1995)
Ras El Ma	35.022524N, 5.206978W; 1633 m	Supramediterranean	Wetland/ peatland	300	0–11000	12 ^{14}C dates	Nour el Bait et al. (2014)
Bab El Karn	37°00′39.77"N, 3°36′14.06"W; 1178 m	Mesomediterranean	Wetland/ peatland	850	0–9000	10 ^{14}C dates	(Cheddadi et al., 2016, 2017)
ODP site 976	36°12′N, 4°18′W; 1108 m below sea level		marine	425*	0–11000	5 ^{14}C dates*	Combourieu Nebout et al. (2009)
MD 95-2043	36°8.6′N, 2°37.3′W; 1841 m below sea level		marine	425*	1200–11000	9 ^{14}C dates*	Fletcher and Sanchez Goñi, (2008)

records from the Sierra Nevada in southern Spain (Table 1). *Cedrus* stack for the last 11,000 cal yr BP for Morocco was built using four Holocene records from the Middle Atlas and Rif mountains (Sidi Ali, Tigalmamine, Ras El Ma and Bab El Karn, see details above). Absolute chronologies of the individual sites are shown in the original publications. *Cedrus* abundance data were resampled (linear interpolation) at 100-yr windows using Analyseries (Paillard et al., 1996) and normalized to z-scores, measuring deviations from the Holocene mean of the utilized record with regard to standard deviations, to stabilize the variance, facilitate their comparison and minimize the local differences within sites. We used the method applied by Power et al. (2008). The z-score of synthetic *Cedrus* abundance from the Sierra Nevada and Morocco for the last ~11,000 cal yr BP were generated averaging the individual *Cedrus* series z-scores used in each region. Maximum and minimum confidence limits for the estimated average values were calculated with the standard deviation for the Sierra Nevada and Morocco *Cedrus* stacks. Standard errors were also calculated (Figs. 3 and 4).

Cedrus data from the two records from the Alboran Sea were also normalized and transformed to z-scores, as well as Holocene paleoclimatic data from NW Africa (terrigenous dust record off NW Africa: de Menocal et al., 2000; δD_{wax}-inferred precipitation NW Africa: Tierney et al., 2017) and an eolian proxy record from the Sierra Nevada (Zr/Th geochemistry data; Jiménez-Espejo et al., 2014). Pearson correlations were made between the different *Cedrus* z-score stacks and to other paleoclimatic records resampled at 100-yr windows to measure their similarities and to evaluate a possible common environmental response to climatic triggers.

Cyclostratigraphic analyses were performed on the Sierra Nevada and Morocco z-score synthetic *Cedrus* stacks. Spectral and wavelet analyses were run on the data using the software PAST (Hammer et al., 2001) with the goal of characterizing the different cyclical periodicities present in the *Cedrus* time series and analyzing their evolution through time. The spectral analyses were done using the REDFIT procedure of Schulz and Mudelsee (2002) under the rectangular window function, a standard value of 2 for the segment parameter and value of 3 for the oversample parameter. Confidence levels at 80% and 90% were also calculated. In the wavelet analyses the basin function of Morlet with a sample interval of 1 was used and the cone of influence and $p = 0.05$ significance level were added.

Cluster-mean backward wind trajectories covering the last 50 years (1970–2019) for the Sierra Nevada area (Padul wetland at 730 masl and the highest Sierra Nevada study site LdRS at 3020 masl) were obtained (Fig. 2). The daily 72-h backward trajectories throughout these 50 years have been calculated by means of the Hybrid Single-Particle Lagrangian Integrated Trajectory (HYSPLIT) model (Hysplit 4.2 version) and the reanalysed meteorological data CDC1 (https://www.ready.noaa.gov/HYSPLIT.php). Since this approach produced a huge amount of data, models including 12-h endpoints and every other backward trajectory endpoint have been used to calculate the clusters and save computational time. The obtained clusters objectively represent different subsets of backward trajectories. The maximum number of these different subsets was established considering the sum of all the cluster spatial variances (total spatial variance, TSV) in each case.

3. Results

The Holocene *Cedrus* record from the Sierra Nevada shows very low abundances in all the study sites, rarely being higher than 1% (Fig. 3A and B). However, the various records show long- and short-term common patterns, which are summarized in the z-scores *Cedrus* stack (Fig. 3). The Sierra Nevada *Cedrus* stack fluctuates between −0.63 and 0.84 values, reached at 7600 and 3600 cal yr BP, respectively. This reconstruction shows long-term changes that could be summarized as an (1) Early- and early-Middle Holocene (11,000–6000 cal yr BP) with significant variability but overall values below zero, (2) a late-Middle and early-Late Holocene (6000–2000 cal yr BP) characterized by an increase first and

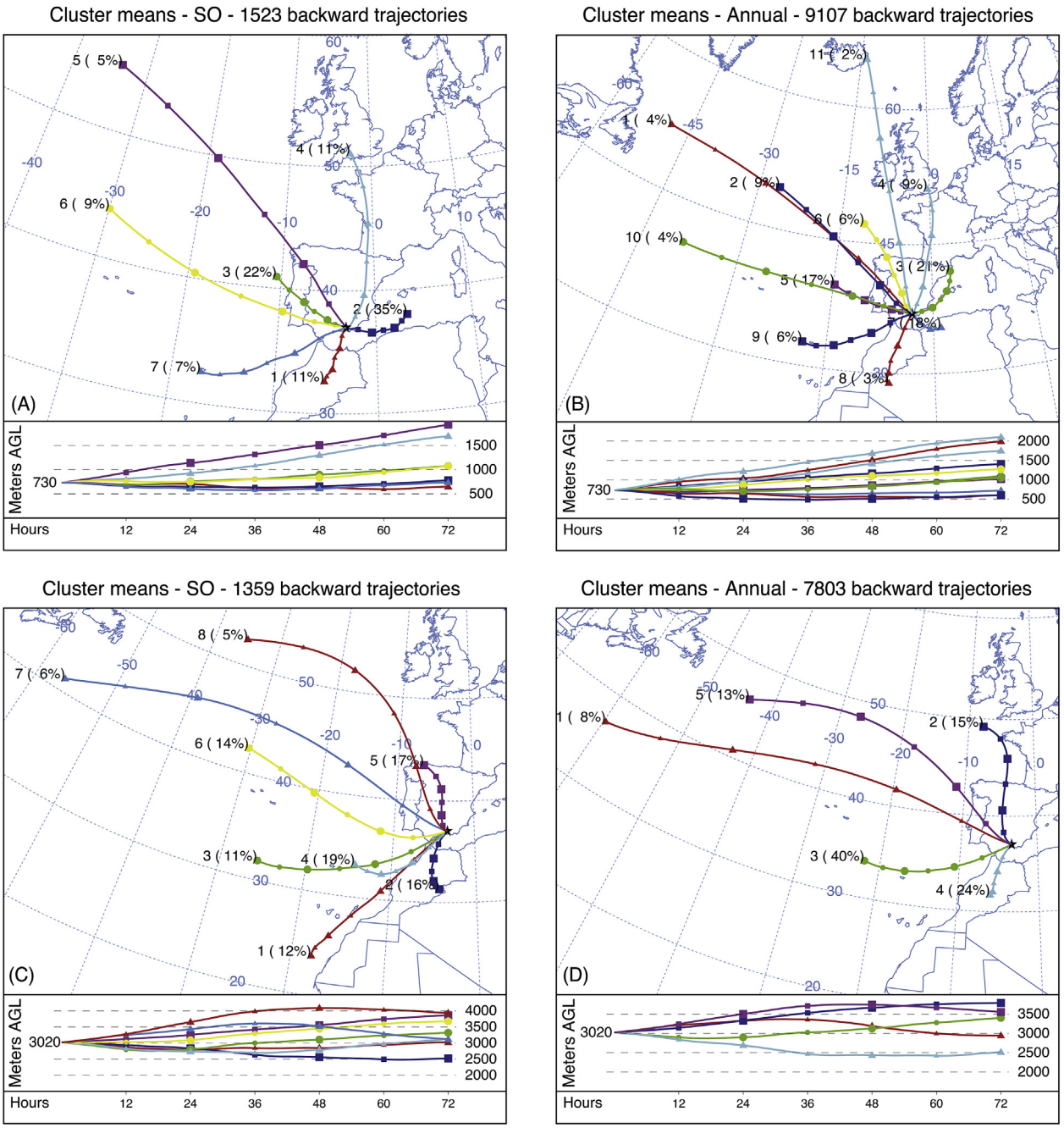

Fig. 2. Cluster-mean backward wind trajectories covering the last 50 years (1970–2019) for the Sierra Nevada area. (A) and (B) are wind trajectories for the Padul wetland (730 masl) and (C) and (D) for the highest Sierra Nevada study site (LdRS, 3020 masl). (A) and (C) represent the cluster-mean backward wind trajectories of September and October, the *Cedrus* pollen production season in north Africa, and (B) and (D) represent the annual cluster-mean backward wind trajectories in the study area. The number of backward trajectories used in the different settings is indicated at the top of each graph. Numbers 1-11 are the ID numbers of the different cluster-mean backward wind trajectories, represented in different colors to facilitate their graphical identification. The contribution of the different clusters to the total backward wind trajectories at the study sites is shown between brackets (%). Images below the maps represent the elevation above ground level (AGL) of the Cluster-mean backward wind trajectories for the previous 72 h. (For interpretation of the references to color in this figure legend, the reader is referred to the Web version of this article.)

maximum values of *Cedrus* between 4200–2300 cal yr BP and (3) a latest Holocene (2000 cal yr BP-present) depicted by a significant decrease in *Cedrus* values (below zero) and an increase at the end of the record with a positive peak between 500 and 300 cal yr BP (Fig. 3).

The synthetic Sierra Nevada *Cedrus* stack also shows short-term millennial- and centennial-scale variability superimposed on the above-mentioned trends. Maximum abundances in *Cedrus* above zero occurred at around 10,200, 9,000, 7,800, 6,800, 5,800, 4200–3,600, 2800–2300 and 500-300 cal yr BP. A strong decrease in *Cedrus* occurred at around 1400–1300 cal yr BP (Fig. 3).

The Holocene *Cedrus* synthetic record from Morocco also shows long- and short-term patterns (Fig. 4). The Early and early-Middle Holocene (11,000–6600 cal yr BP) is characterized by low but increasing z-score values generally below zero. The late-Middle and most of the Late Holocene (6600–1300 cal yr BP) is depicted by overall high values above zero and maxima at 6200 and 3100 cal yr BP. The latest Holocene (1300 cal yr BP – present) is depicted by

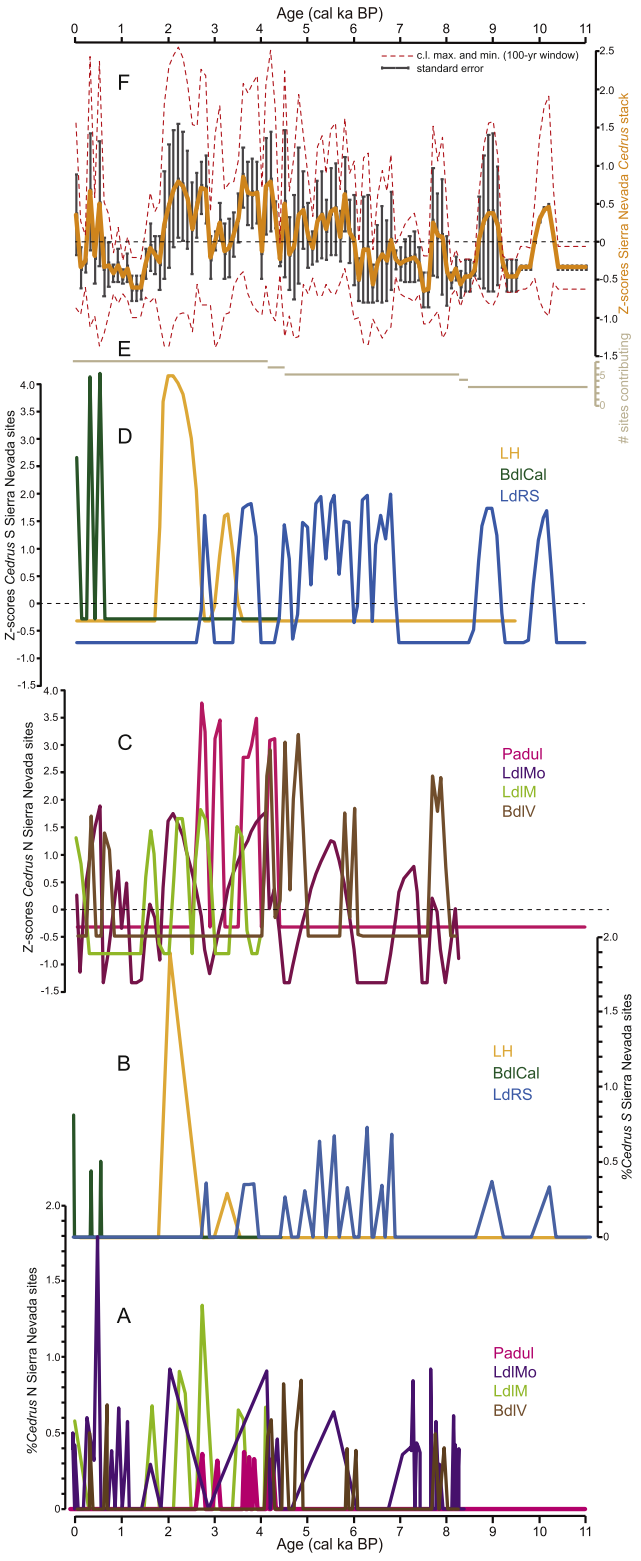

Fig. 3. Reconstruction of *Cedrus* abundance stack for the Sierra Nevada during the last ~11,000 cal yr BP, from seven sites shown in Fig. 1A. (A) *Cedrus* abundances in percentage in the studied records from the north face of the Sierra Nevada plus Padul (see Fig. 1 caption for explanation of the acronyms). (B) *Cedrus* abundances in percentage in the studied records from the south face of the Sierra Nevada (see Fig. 1 caption for explanation of the acronyms). (C) Z-scores of the north face Sierra Nevada *Cedrus* records and Padul. (D) Z-scores of the south face Sierra Nevada *Cedrus* records. (E) The number of sites (grey line) contributing to the *Cedrus* regional summary. (F) Z-score synthetic *Cedrus* stack from Sierra Nevada, S Spain (100-yr window). Maximum and minimum confidence limits (c.l.) were calculated with the standard deviation. Standard errors are also shown.

decreasing values below zero and a slight increase to positive values between 500 and 100 cal yr BP. Millennial- and centennial-scale variability is also appreciated in the Morocco *Cedrus* stack. *Cedrus* peaks (and subtle peaks, between parentheses) are recorded at ~10,100, (9000), 8,200, (6900), 6,200, (4400), 3500–3,100, 2,300, (1900) and 200-100 cal yr BP (Fig. 4).

Comparison and Pearson correlations were performed between the Sierra Nevada *Cedrus* stack and individual *Cedrus* records from N Morocco, Morocco Holocene *Cedrus* stack and *Cedrus* records from the Alboran Sea at 100-yr windows (Table 2; Fig. 5). Positive correlations were obtained between the Sierra Nevada and Moroccan records, some of them being significant ($r > 0.32$; $p < 0.01$) such as between Sierra Nevada and Morocco stack ($r > 0.4$; $p < 0.01$). Little positive correlation ($r = 0.19$; $p = 0.04$) or no correlation ($r = -0.05$; $p = 0.59$) were obtained between the Sierra Nevada *Cedrus* stack and ODP site 976 and Bab El Karn records, respectively. The Bab El Karn record shows negative correlations to most of the sites, especially with the Tigalmamine ($r = -0.72$; $p < 0.01$) and Ras El Ma ($r = -0.35$; $p < 0.01$). The Moroccan sites all correlate positively between each other except with Bab El Karn. With respect to the marine records, MD95-2043 correlates positively with all the records, particularly with the Tigalmamine ($r = 0.58$; $p < 0.01$) and Morocco ($r = 0.5$; $p < 0.01$) and Sierra Nevada ($r = 0.39$; $p < 0.01$) stacks, and ODP site 976 shows little correlations with any of the sites except for the positive correlation ($r = 0.45$; $p < 0.01$) with the data from Bab El Karn.

Our Pearson correlation analysis also compares the Sierra Nevada *Cedrus* stack and climate and aridity-related dust from W Africa (terrigenous dust record off NW Africa: de Menocal et al., 2000; δD_{wax}-inferred precipitation NW Africa: Tierney et al., 2017), and eolian proxy data from the Sierra Nevada (Zr/Th record from the Laguna de Río Seco; Jiménez-Espejo et al., 2014) (Table 3; Fig. 6). This analysis shows negative correlations ($r = -0.38$; $p < 0.01$) for precipitation reconstructions, and positive ($r > 0.35$; $p < 0.01$) correlations with climate related eolian dust in both NW Africa and Sierra Nevada records. Strong correlations are obtained between climate in NW Africa (i.e., precipitation) and dust flux in Africa ($r = -0.7$; $p < 0.01$) and Sierra Nevada ($r = -0.72$; $p < 0.01$) and between the dust records from the two studied regions ($r = 0.96$; $p < 0.01$).

Spectral analysis on the Sierra Nevada z-scores *Cedrus* pollen stack shows statistically significant (above the 80 and 90% confidence level) spectral peaks at periodicities between ~520 and 550, 1050 and 1600 years (Fig. 7). Spectral analysis on the Morocco z-scores *Cedrus* pollen stack depicts statistically significant spectral peaks with periodicities of ~550–650, 900-1000, 1500 and 2100 years. The wavelet analysis of the Sierra Nevada data time-series displays a change in the cyclical periodicities from an Early and early-Middle Holocene dominated by a ~1000-yr cycle to a late-Middle Holocene and Late Holocene dominated by ~1600-2000-yr cyclicity. Wavelet analysis of the Morocco *Cedrus* data time-series also shows a change in periodicities at around 6000 cal yr BP, with the muting of the ~1000-yr cyclicity in the late-Middle Holocene and Late Holocene.

Two main groups of backward wind trajectories were obtained using the Hybrid Single-Particle Lagrangian Integrated Trajectory (HYSPLIT): 1) September and October (SO; Fig. 2A and C), since *Cedrus atlantica* releases pollen during those two months, and 2) annual periods (Fig. 2B and D), to assess the wind pattern all year round. A SSW wind component during September and October is relatively important (>10%) at the study sites. This contribution changes with the elevation when annual periods are considered, ranging from 24% at 3020 masl to 3% at 730 masl. Lower elevations (Padul wetland) will also register the accumulated effect of the catchment basin that extends to higher Sierra Nevada areas.

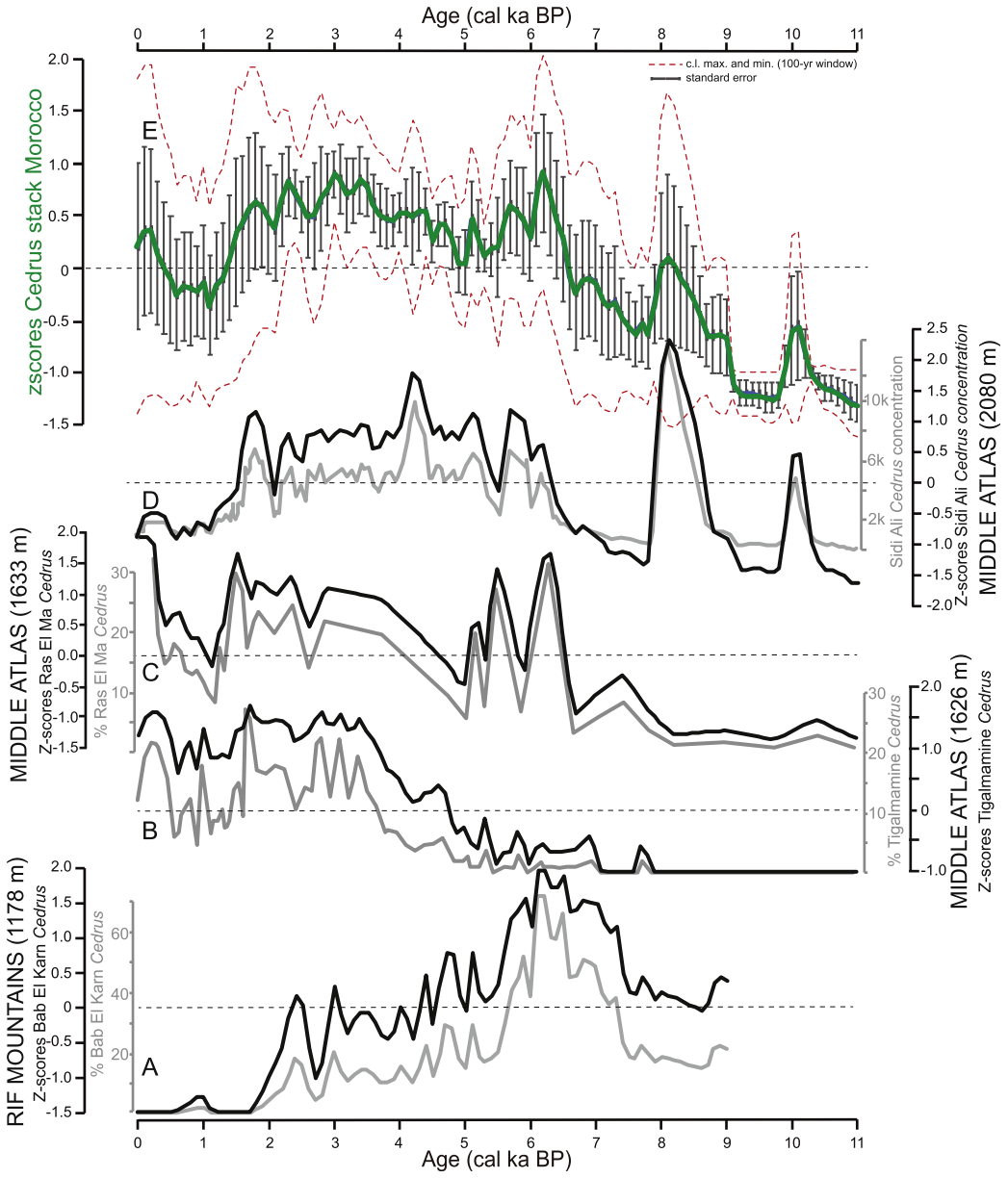

Fig. 4. Reconstruction of *Cedrus* abundance stack for Morocco during the last ~11,000 cal yr BP, from four sites shown in Fig. 1A. (A) Percentages and z-scores of *Cedrus* record from Bab El Karn (Rif Mountains, Morocco; Cheddadi et al., 2017). (B) Percentages and z-scores of *Cedrus* record from Tigalmamine (Middle Atlas, Morocco; Lamb and van der Kaars, 1995). (C) Percentages and z-scores of *Cedrus* record from Ras El Ma (Middle Atlas, Morocco; Nour el Bait et al., 2014). (D) Concentration and z-scores of *Cedrus* record from Sidi Ali (Middle Atlas, Morocco; Campbell et al., 2017). (E) Z-score synthetic *Cedrus* stack from Morocco (100-yr window). Maximum and minimum confidence limits (c.l.) were calculated with the standard deviation. Standard errors are also shown.

Table 2
Pearson correlations between the normalized z-scores of Holocene (11,000-0 cal yr BP) *Cedrus* records from northern Morocco (Sidi Ali: Lamb et al., 1995; Campbell et al., 2017; Tigalmamine: Lamb and van der Kaars, 1995; Ras El Ma: Nour el Bait et al., 2014 and Bab El Karn: Cheddadi et al., 2017), the synthetic z-score stacks from Morocco and Sierra Nevada and the marine core records from the Alboran Sea MD95-2043 (Fletcher and Sanchez Goñi, 2008) and ODP 976 (Combourieu-Nebout et al., 2009). All records were previously resampled by linear interpolation at 100-yr window (see methods for further explanation). In orange and red color are positive correlations between $r = 0.25–0.50$ and higher than 0.50, respectively. In light and dark blue are negative correlations between $r = -0.25$ - -0.50 and higher than −0.50, respectively.

	Sidi Ali	Tigalmamine	Ras El Ma	Bab El Karn	Morocco	Sierra Nevada	MD95-2043	ODP 976
Sidi Ali		0.00090	5.51E-05	0.77	1.24E-21	0.00014	0.0016	0.12
Tigalmamine	0.31		4.24E-24	4.32E-16	2.94E-15	5.95E-04	1.93E-10	0.073
Ras El Ma	0.37	0.78		0.00054	2.29E-29	6.17E-04	1.55E-06	0.42
Bab El Karn	0.03	−0.72	−0.35		0.99	0.59086	8.65E-02	7.08E-06
Morocco	0.75	0.66	0.82	0.0004		8.85E-06	1.29E-07	0.11
Sierra Nevada	0.35	0.32	0.32	−0.05	0.40		4.98E-05	0.042
MD95-2043	0.31	0.58	0.46	−0.19	0.50	0.39		0.094
ODP 976	0.15	−0.17	0.07	0.45	0.15	0.19	0.17	

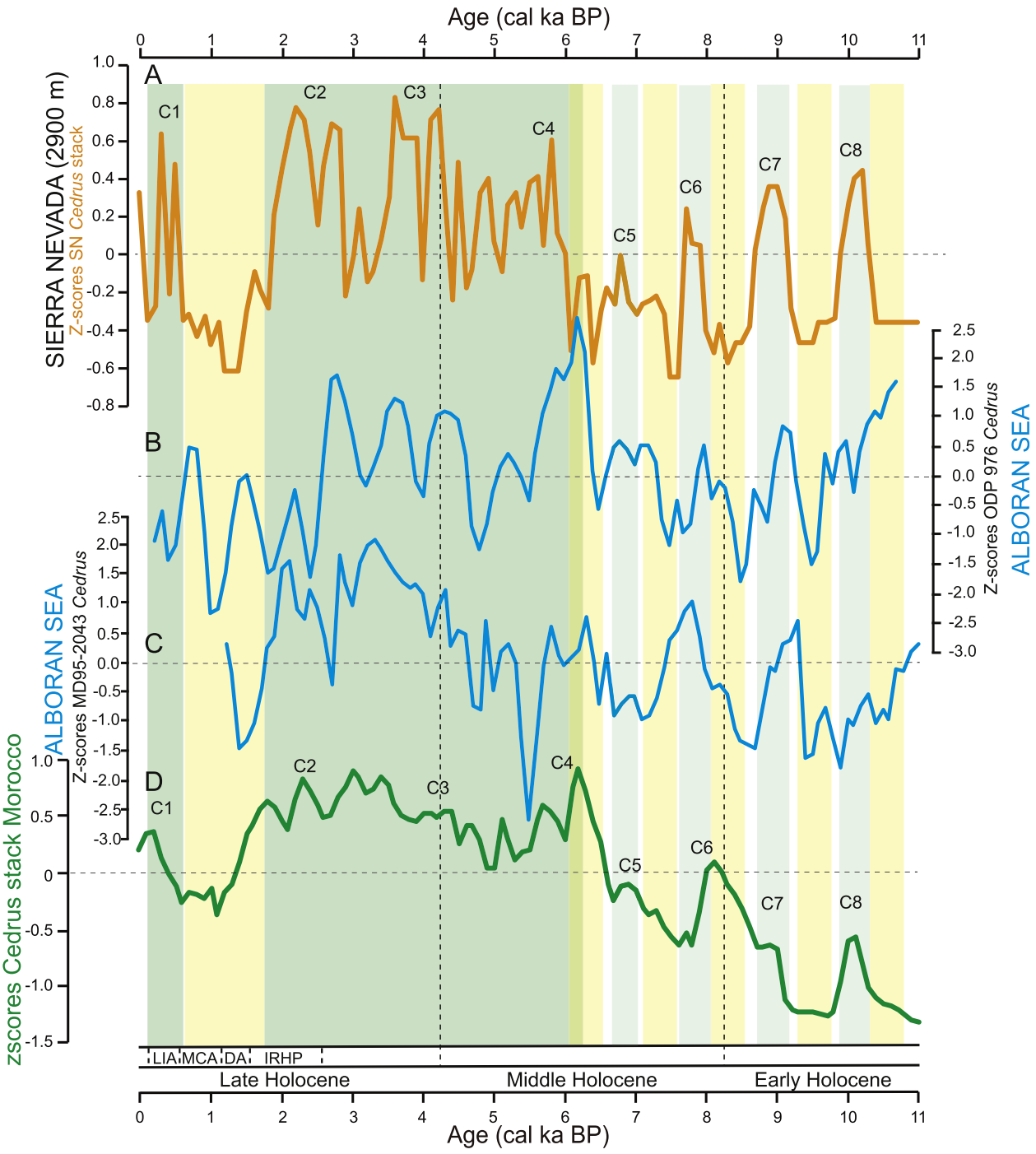

Fig. 5. Comparison of *Cedrus* records from the western Mediterranean area. (A) Sierra Nevada z-scores Holocene *Cedrus* stack. C1-C8 correspond to peaks in *Cedrus*. (B) Z-scores of *Cedrus* record from Alboran Sea ODP 976 site (Combourieu-Nebout et al., 2009). (C) Z-scores of *Cedrus* record from Alboran Sea MD95-2043 site (Fletcher and Sanchez Goñi, 2008). (D) Morocco z-scores Holocene *Cedrus* stack. C1-C8 correspond to peaks in *Cedrus* that could correspond to the ones detected in Sierra Nevada. Green and yellow shadings highlight high and low abundances of *Cedrus*, respectively, in Sierra Nevada and the western Mediterranean. IRHP, DA, MCA and LIA are abbreviations for Iberian-Roman Humid Period, Dark Ages, Medieval Climate Anomaly and Little Ice Age, respectively. (For interpretation of the references to color in this figure legend, the reader is referred to the Web version of this article.)

4. Discussion

4.1. Long-term climate control of the Holocene Cedrus pollen record in the western Mediterranean

This synthetic study using pollen records from Morocco and Sierra Nevada in the western Mediterranean shows similar *Cedrus* dynamics (positive correlation of $r = 0.4$; $p < 0.01$; Table 2), mostly related to climate change at long- and short-timescales during the Holocene (Fig. 6). This indicates that the composite windblown *Cedrus* record from the S Europe sites could be used as a proxy for environmental and climate change in northern Africa, if analyzed carefully. Below we discuss the main changes observed in the *Cedrus* abundance in the western Mediterranean area.

Table 3
Pearson correlations between the normalized z-scores of Holocene (11,000-0 cal yr BP) *Cedrus* records from Sierra Nevada and Morocco, climate and dust records from northern Africa and Sierra Nevada. δD_{wax}-inferred precipitation NW Africa (Tierney et al., 2017). Terrigenous dust record off NW Africa (de Menocal et al., 2000) and eolian proxy record from the Sierra Nevada (Zr/Th geochemistry data; Jiménez-Espejo et al., 2014). In orange and red color are positive correlations between $r = 0.25–0.50$ and higher than 0.50, respectively. In light and dark blue are negative correlations between $r = -0.25$ - -0.50 and higher than -0.50, respectively.

	Precip. Africa	Dust Africa	*Cedrus* Morocco	*Cedrus* SN	Dust Sierra Nevada
Precip. Africa		1.10E-16	1.50E-06	6.07E-05	3.38E-18
Dust Africa	−0.70		1.91E-18	5.13E-05	3.48E-62
Cedrus Morocco	−0.45	0.73		8.37E-06	8.46E-20
Cedrus Sierra Nevada	−0.38	0.38	0.42		0.0002
Dust Sierra Nevada	−0.72	0.96	0.74	0.35	

Cedrus abundance was generally low in the western Mediterranean area during the Early- and early-Middle Holocene ~11,000–6000 cal yr BP, as indicated by *Cedrus* records from Morocco, the Sierra Nevada and the Alboran Sea, which show overall low values below zero (Figs. 5 and 6). *Cedrus* is restricted to cool-cold and humid-subhumid climates and is very sensitive to drought conditions (Cheddadi et al., 2009; Linares et al., 2011). Perhaps its distribution was reduced to high elevations during the Early and early-Middle Holocene due to very warm summers with high evapo-transpiration rates during maxima in summer insolation (Cheddadi et al., 2016; Laskar et al., 2004). Previous studies have shown that temperature maxima (Samartin et al., 2017; Català et al., 2019) and highest elevation of treeline in the western Mediterranean area occurred between ~10,500 and 7000–6000 cal yr BP (Cheddadi et al., 1998; Anderson et al., 2011; Jiménez-Moreno and Anderson, 2012; Campbell et al., 2017; Ramos-Román et al., 2018a,b). This is indicated in the pollen records by the abundance of temperate tree species, such as deciduous *Quercus* and the highest tree (e.g., *Pinus*) abundance in high elevation alpine records (Anderson et al., 2011; Jiménez-Moreno and Anderson, 2012; Mesa-Fernández et al., 2018). However, different authors have interpreted the vegetation sequence in terms of both precipitation maxima (Fletcher and Sánchez Goñi, 2008; Jalut et al., 2009; Dormoy et al., 2009; Combourieu Nebout et al., 2009; Anderson et al., 2011; Jiménez-Moreno and Anderson, 2012; Cheddadi et al., 2016; Ramos-Román et al., 2018a,b) and minima (Cheddadi et al., 1998; Nour el Bait et al., 2014) for the Early and early-Middle Holocene. *Cedrus*, with its cold-humid preference (Cheddadi et al., 1998) is most abundant during the Middle Holocene in Morocco in the Rif Mountains (see the Bab El Karn record; Cheddadi et al., 2016, 2017, Fig. 4) and during the late-Middle and Late Holocene in the Middle Atlas Mountains (Lamb and van der Kaars, 1995; Lamb et al., 1999; Nour et Bait et al., 2014; Campbell et al., 2017; see negative correlations in Table 2; Fig. 4). These differences could be explained by different site vegetation sensitivity to precipitation and/or humidity depending on many factors such as elevation or orientation (Anderson et al., 2011; Ramos-Román et al., 2018a). For example, soil humidity and plant evapotranspiration can be quite different under the same climatic regime depending on elevation; if the site is located at low elevation, subjected to higher evaporation, or at higher elevation, subjected to higher precipitation and lower evaporation. In any case, most of the synchronous paleoclimatic records from the Mediterranean area show enhanced fall/winter precipitation related to maximum summer insolation that could have boosted land/sea temperature contrast triggering higher fall/winter rainfall (Meijer and Tuenter, 2007). However, high summer temperatures and evaporation rates probably limited the abundance and distribution of *Cedrus* to high-elevations in Morocco.

Cedrus pollen increased in the western Mediterranean area during the late-Middle and early-Late Holocene (~6000–2000 cal yr BP), reaching maximum occurrences between 4200–2300 cal yr BP (Fig. 5). *Cedrus* probably expanded during a period favored by diminishing summer insolation, leading to a decrease in summer water evaporation and plant evapotranspiration (Tzedakis, 2007). Thus, *Cedrus* most likely thrived as climate cooled, especially during the summer, when humidity persisted and evaporation was lower. This follows other observations on the effect of changing insolation dynamics on increases in mid- and high-altitude conifers such as *Cedrus* or *Abies* during the late phase of interglacials (van der Hammen et al., 1971; Combourieu Nebout, 1993; Tzedakis, 2007; Jiménez-Moreno et al., 2013). This evolving vegetation pattern is most clear in the Holocene Tigalmamine pollen record, where a pre-temperate, warm-dry phase of open woodland characterized by evergreen *Quercus* was replaced by a temperate, warm-humid phase with deciduous *Quercus* and later with a cool-humid montane and coniferous forest including *Cedrus* after 5000 cal yr BP (Lamb and van der Kaars, 1995; Cheddadi et al., 1998). Another factor that could have accounted for the increase in *Cedrus* abundance was probably its displacement towards lower elevations due to climate cooling, occupying wider distribution areas at the bottom of the mountain ranges (Cheddadi et al., 2016). The only record from our study that shows a different pattern of *Cedrus* is the Bab El Karn record, which documents a decline at that time (Cheddadi et al., 2017) and no correlation or negative correlation to the other Moroccan and *Cedrus* stack records (Table 2; Fig. 4), probably due to local site particularities (see explanation above and in sections 4.4 and 4.5 below).

Our study of *Cedrus* is consistent with previous research documenting a transition towards a climate cooling, a change in atmospheric configuration and more regional aridity since the Middle Holocene ~6000 cal yr BP in the western Mediterranean, which was intensified in the Late Holocene most likely related to decreasing summer insolation (de Menocal et al., 2000; Dormoy et al., 2009; Jalut et al., 2009; Fletcher et al., 2013; Jiménez-Espejo et al., 2014; Ramos-Román et al., 2018a, 2018b; Bell et al., 2019). *Cedrus* abundances also parallels an expansion of Ericaceae heathlands since the Middle Holocene (~6000 cal yr BP) in the Iberian Peninsula (Fletcher and Sánchez Goñi, 2008; Combourieu-Nebout et al., 2009; Carrión et al., 2010; Morales-Molino et al., 2013; Oliveira et al., 2016; Ramos-Román et al., 2018a; Gomes et al., 2020). Heathlands grow well under high atmospheric humidity and climates characterized by little seasonal precipitation contrast (Ojeda et al., 1998). Thus, heathland expansion also supports our hypothesis of reduced seasonality and more continuous soil humidity (particularly during summer) since the Middle Holocene in the western Mediterranean.

This trend is reversed between ~2000 and 600 cal yr BP with declining *Cedrus* in the Sierra Nevada z-scores stack (Fig. 3). Absolute minima occurred between 1400–1300 cal yr BP, coinciding with the Dark Ages (DA) and Medieval Climate Anomaly (MCA) (1550-650 cal yr BP; Moreno et al., 2012). A similar declining trend and minimum at ~1200 cal yr BP occurred in all the *Cedrus* pollen records from Morocco and thus the z-scores stack, as well as pollen records from the Alboran Sea (Fig. 5). We interpret this decline in

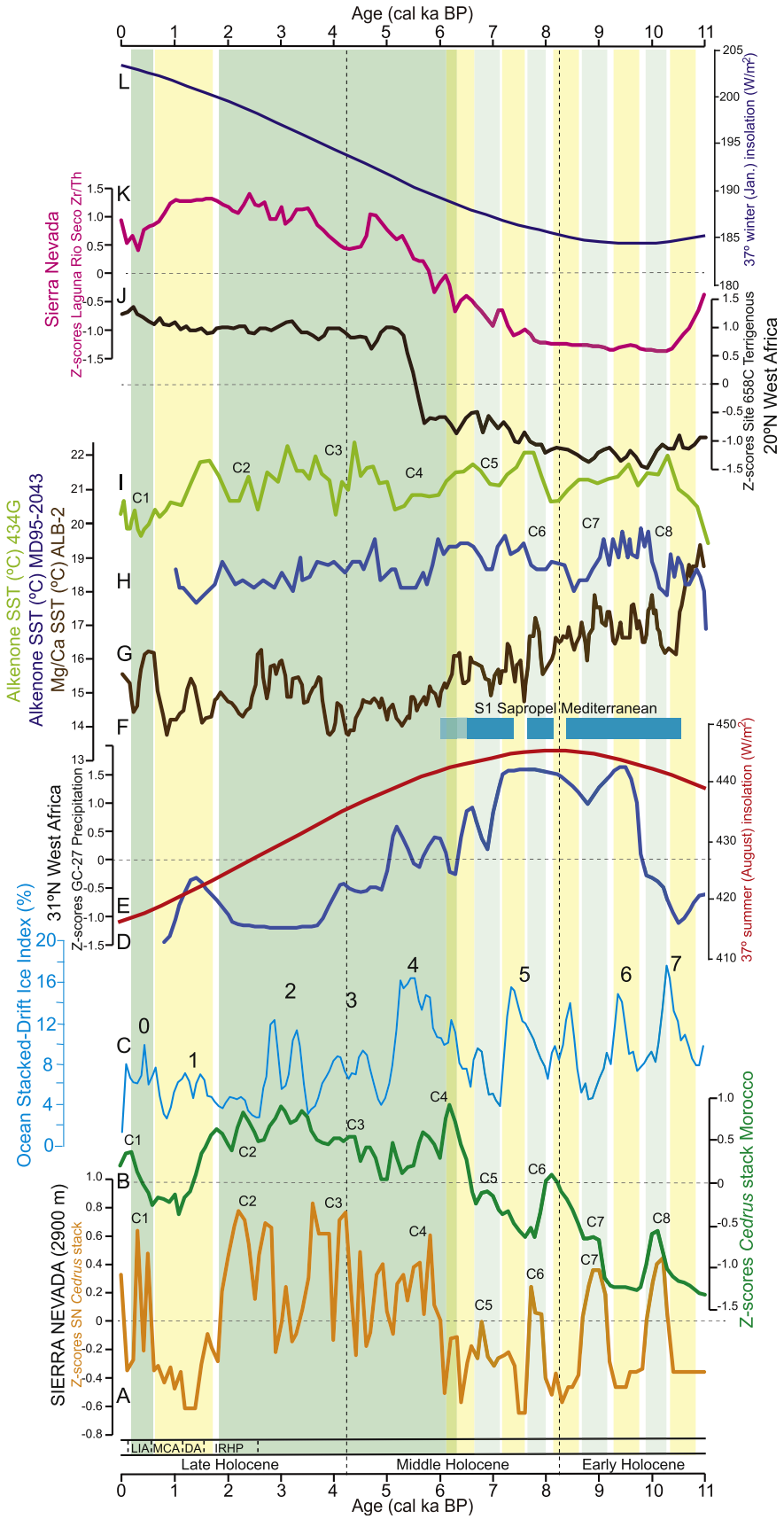

Fig. 6. *Cedrus* records and climate for the last 11,000 cal yr BP in the western Mediterranean area. (A) Sierra Nevada z-scores Holocene *Cedrus* stack. C1-C8 correspond to peaks in *Cedrus*. (B) Morocco z-scores Holocene *Cedrus* stack. C1-C8 correspond to peaks in *Cedrus* that could correspond to the ones detected in Sierra Nevada. (C) Ocean stacked ice-rafting debris (IRD) from the North Atlantic (Bond et al., 2001). Numbers 0-7 indicate cold climate events. (D) Z-scores of dDwax reconstructed mean annual precipitation from marine core

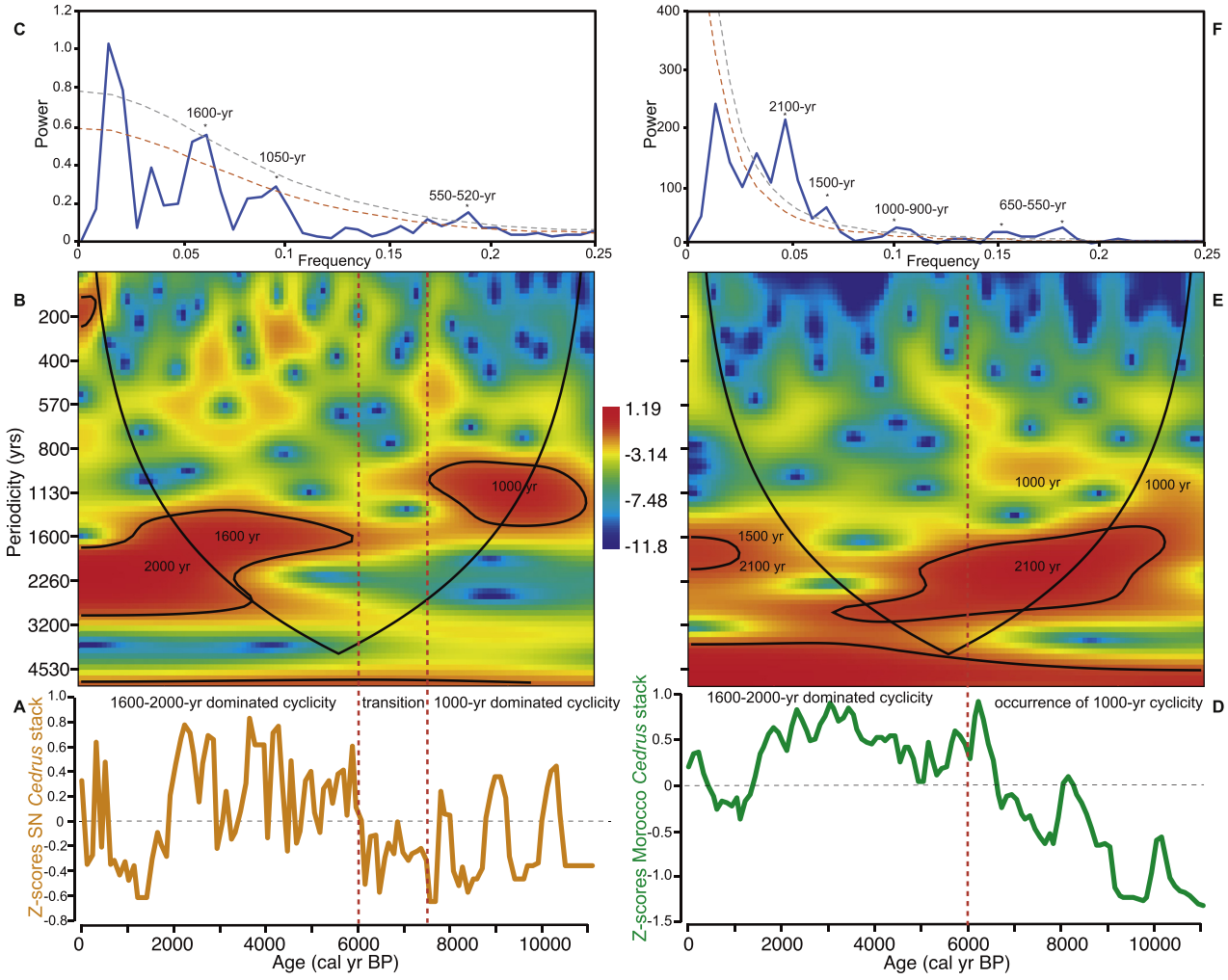

Fig. 7. Wavelet and spectral cyclostratigraphy analysis of the Sierra Nevada Cedrus stack. (A) Sierra Nevada *Cedrus* stack indicating periods with characteristic cyclical variability. (B) Wavelet analysis of the Sierra Nevada *Cedrus* stack. (C) Spectral analysis of Sierra Nevada *Cedrus* stack. Confidence levels at 80% (orange line) and 90% (grey line) and the statistically significant periodicities above the 80% are shown. (D) Morocco *Cedrus* stack indicating periods with characteristic cyclical variability. (E) Wavelet analysis of the Morocco *Cedrus* stack. (F) Spectral analysis of Morocco *Cedrus* stack. Statistical analyses were done using Past software 3.20 (Hammer et al., 2001). (For interpretation of the references to color in this figure legend, the reader is referred to the Web version of this article.)

Cedrus in the western Mediterranean area as a result of enhanced and persistent aridity or droughty conditions at that time, which probably generated forest decline or dieback. However, human influence on the environments in the study area enhanced in the last two millennia (Nour el Bait et al., 2014; Cheddadi et al., 2014; Campbell et al., 2017; Ramos-Román et al., 2018b) and the significant decrease in *Cedrus* observed at that time could be due to the combination of extreme drought and to the intensification of human activity (Campbell et al., 2017). Support for enhanced aridity at that time includes decreases in *Quercus* forest species in the Sierra Nevada around 1800–700 cal yr BP (Laguna de la Mula; Jiménez-Moreno et al., 2013; Borreguil de la Caldera: Ramos-Román et al., 2016), being especially arid at ~1300 cal yr BP (Padul-15-05; Ramos-Román et al., 2018b) and degradation and opening of forest cover in Morocco between 1300 and 580 cal yr BP (Sidi Ali; Campbell et al., 2017). Previous studies based on lake levels and organic and inorganic elemental geochemical analyses also interpreted dry climate conditions during the DA and MCA in the western Mediterranean area (Magny et al., 2004; Moreno et al., 2012; García-Alix et al., 2020), supporting our interpretations. Persistent positive NAO phases are blamed for the overall reduction in precipitation and increased aridity at this time in the region (Trouet et al., 2009; Moreno et al., 2012; Ramos-Román et al., 2016). However, higher temperatures are also interpreted for the study area during the DA and MCA periods (Nieto-Moreno et al., 2013; García-Alix et al., 2020), which would also have increased

site GC-27 (NW Africa) (Tierney et al., 2017). (E) Summer (August) insolation values at 37°N (Laskar et al., 2004). (F) Blue shaded areas show the S1 sapropel boundaries in the Adriatic Sea by Filippidi and De Lange (2019). Note the transition at the end of the Sapropel deposition between 6000–6600 cal yr BP coinciding with the *Cedrus* record. (G) Sea Surface Temperature (SST) reconstructed from *G. bulloides* Mg/Ca ratios from marine core ALB-2 (Alboran Sea; Català et al., 2019). (H) SST (°C) reconstructed from alkenones from marine sediment core MD95-2043 (Cacho et al., 1999). (I) SST (°C) reconstructed from alkenones from marine sediment core 434G (Rodrigo-Gámiz et al., 2014a,b). C1-C8 could correspond to peaks in *Cedrus* detected in Sierra Nevada. (J) Z-scores of terrigenous (%) dust input in marine core 658C from NW Africa (deMenocal et al., 2000). (K) Z-scores of Zr/Th dust proxy record from Sierra Nevada (Jiménez-Espejo et al., 2014). (L) Winter (January) insolation at 37°N (Laskar et al., 2004). Green-blue and yellow shadings highlight high and low abundances of *Cedrus*, respectively, in Sierra Nevada and the western Mediterranean. IRHP, DA, MCA and LIA are abbreviations for Iberian-Roman Humid Period, Dark Ages, Medieval Climate Anomaly and Little Ice Age, respectively. (For interpretation of the references to color in this figure legend, the reader is referred to the Web version of this article.)

evaporation and increase water stress in *Cedrus* and other humidity/drought sensitive plants, particularly during summer.

The Sierra Nevada *Cedrus* stack increases substantially at the end of the record, peaking between 500 and 300 cal yr BP (Fig. 5). A simultaneous increase in *Cedrus* occurs in both the Morocco stack and marine record from the Alboran Sea (ODP site 976; Combourieu Nebout et al., 2009, Fig. 5), confirming this is a regional feature of the western Mediterranean. The timing suggests that the increase in *Cedrus* could have been induced by enhanced humidity during the Little Ice Age (LIA; ~650 to 100 cal yr BP). This is supported by previous studies that show varying but overall humid climate conditions during the LIA in the western Mediterranean area (Morellón et al., 2011; Oliva et al., 2018; Zielhofer et al., 2019). More humid conditions would have benefited *Cedrus* growth and distribution in Morocco, as shown by the Middle Atlas *Cedrus* tree ring record (Esper et al., 2007). Accompanying this were colder conditions during the LIA (Campbell et al., 2017; Oliva et al., 2018; García-Alix et al., 2020). Overall colder conditions could have positively impacted the *Cedrus* growing season and modulated the intensity of soil evaporation during summer drought. This climatic cooling also probably forced *Cedrus* woodlands towards lower elevations, expanding its areal distribution in the Middle Atlas and Rif mountain areas.

González-Sampériz et al. (2010) and Postigo-Mijarra et al. (2010) have suggested the possibility that local populations of *Cedrus* survived in refuge areas in the Iberian Peninsula until some point during the late Glacial and the Holocene. Even though this hypothesis cannot be discounted, *Cedrus* macroremains have not been found from Holocene sedimentary records from within its potential distribution, such as the Sierra Bermeja in S Spain (Olmedo-Cobo et al., 2017). However, negative evidence cannot be conclusive, and until remains are found from this area we must remain skeptical of its occurrence.

4.2. Millennial-scale climate and Cedrus variability

Short-term millennial- and centennial-scale variability occur in the *Cedrus* pollen stack from Sierra Nevada, superimposed on the long-term insolation-related Holocene climate changes. Peaks in *Cedrus* abundance occurred ~10,200, 9,000, 7,800, 6,800, 5,800, 4200–3,600, 2800–2300 and 500-300 cal yr BP (Figs. 5 and 6). Similar short-term variability is observed in the Morocco *Cedrus* stack with obvious peaks at ~10,100, 8,200, 6,200, 3500–3,100, 2300–1900 and 200-100 cal yr BP. Smaller peaks occur at 9,000, 6900 and 4400 cal yr BP. This short-term variability is also recorded in the Alboran Sea *Cedrus* records (Fletcher et al., 2013; Combourieu Nebout et al., 2009, Fig. 5). Therefore, even considering potential age differences due to radiocarbon dating uncertainties, the *Cedrus* records from western Mediterranean show synchronous expansions at ~10,200 (C8), 9000 (C7), 8200–7800 (C6), 6900-6800 (C5), 6200–5800 (C4), 4400–4200 (C3), 2300 (C2) and 500-200 (C1) cal yr BP (Figs. 5 and 6).

Millennial-scale *Cedrus* expansions and contractions in Morocco, also reflected in the pollen records from Sierra Nevada, were undoubtedly produced by climatic variability (Cheddadi et al., 2009, 2017; Zielhofer et al., 2017, 2019). In this study we show that expansions generally occurred during well-known cold [e.g., ~8.2 (C6) and 4.2 ka (C3) events, LIA (C1)] and/or humid [e.g., IRHP (C2), LIA (C1)] events in the western Mediterranean or North Atlantic areas (Fig. 6). Persistence of both colder and/or wetter conditions would have reduced water stress and benefitted the reproduction and growth of *Cedrus* species (Cheddadi et al., 2017), especially during summers and throughout the Early Holocene peak in summer insolation. In this respect, an agreement exists between SST records from the Alboran Sea and *Cedrus* variability in the western Mediterranean, with peaks in *Cedrus* (C1-8) occurring during cold SST conditions (Fig. 6). A slight age discrepancy is recorded between the Sierra Nevada and Morocco *Cedrus* stacks during the C6 *Cedrus* peak related to the ~8.2 ka cooling event. This peak is recorded just a few centuries later in Sierra Nevada, around 7800 cal yr BP. We believe this is not due to a lag in the pollen transport between Morocco and Sierra Nevada but to age uncertainties in the radiocarbon record. However, support for a more modern age for the expression of this cold event in the Mediterranean area comes from different records in the SW and central Mediterranean, which show negligible or limited paleoclimatic expression to the North Atlantic 8.2 ka cooling event (Frisia et al., 2006; Dormoy et al., 2009), but a marked paleoclimatic variation at ~7.7 ka (Magny et al., 2007; Holzwarth et al., 2010). Covariation between the Sierra Nevada and Morocco *Cedrus* records is clearer for the last 7000 cal yr BP (C5-C1), and agrees with Zielhofer et al. (2019), who related *Cedrus* enhancements in the Sidi Ali pollen record from the Middle Atlas in N Morocco to declines in summer temperatures at short-scale millennial-scale variability.

A number of Holocene paleoclimatic studies suggest linkages between millennial-scale climate variability in the western Mediterranean and the North Atlantic (Bond et al., 2001), with cold events in the North Atlantic often occurring with cold and/or arid events in the western Mediterranean (e.g., Dormoy et al., 2009; Jiménez-Moreno et al., 2013; Ramos-Román et al., 2018a, 2018b; Zielhofer et al., 2019). Although our *Cedrus* record shows the same number of variations with similar duration, their climatic affinity to either cold (events from 0 to 7; Bond et al., 2001) or warm events in the N Atlantic is not completely clear (Fig. 6). For example, the *Cedrus* record peaks of C4 (6200–5800 cal yr BP), perhaps C3 (4400–4200 cal yr BP), and C1 (LIA) are roughly synchronous with cold Bond events 4, 3 and 0 but the rest of the *Cedrus* peaks (i.e., C8, C7 or C5) seem to occur during predominant warm conditions in the N Atlantic. This can be true if the strength of climate teleconnections between the two regions vary in time, or the *Cedrus* record is more dependent on precipitation or the varying combination of both temperature-precipitation relations.

This study shows a maximum in *Cedrus* (C3) during the 4.2 ka climatic event (Fig. 6). Regionally, this event has been interpreted as cold (e.g., shown in SST records in Fig. 6; Cacho et al., 1999; Rodrigo-Gámiz et al., 2014; Català et al., 2019) but also dry (Lamb and van der Kaars, 1995; Arz et al., 2006; Carrión et al., 2007; Fletcher et al., 2007; Jalut et al., 2009; Magny et al., 2009; Jiménez-Moreno and Anderson, 2012; Ramos-Román et al., 2018a, 2018b; Di Rita and Magri, 2019). Therefore, temperature must have had a major role controlling *Cedrus* expansions and contractions, at least in the Middle-Late Holocene, with lower soil evaporation and evapotranspiration during cold events benefiting the growth and development of this conifer species under arid conditions. A second peak in *Cedrus* in recorded between 3800–3600 cal yr BP in the Sierra Nevada record (Fig. 6), which could be related to a secondary phase of this climatic event, also recorded at around 3800 cal yr BP in the lipid biomarker temperature record from Laguna de Río Seco (Toney et al., 2020) and other paleoclimatic records from the Mediterranean area (see syntheses in Bini et al., 2019 and Di Rita and Magri, 2019). However, there is not an equivalent peak in the Morocco record.

The C2 peak in *Cedrus* around 2300 cal yr BP occurred during the Iberian–Roman Humid Period (IRHP; between 2600 and 1600 cal yr BP; Martín-Puertas et al., 2009) (Fig. 6), previously regionally identified as an especially humid (Fletcher et al., 2013; Combourieu-Nebout et al., 2009; Martín-Puertas et al., 2009; Nieto-Moreno et al., 2013; Jiménez-Moreno et al., 2013; Ramos-Román et al., 2016, 2018b; Mesa-Fernández et al., 2018). In this case, enhanced precipitation must also have been an important

driver for *Cedrus* expansion in the area. Perhaps the combination of high precipitation and colder conditions at that time (shown in SST records in the Albora Sea; Cacho et al., 1999; Rodrigo-Gámiz et al., 2014a) triggered one of the maxima in *Cedrus* for the entire Holocene period.

Short-term millennial- and centennial-scale variability in the *Cedrus* record from the Sierra Nevada are cyclical (Figs. 6 and 7). Visual as well as spectral and wavelet analyses of the Sierra Nevada and Morocco *Cedrus* stacks show cyclicities that evolve through time. The Early and early-Middle Holocene in the Sierra Nevada and Morocco records is mostly characterized by cyclical periodicities of ~1000 and 2100 years in *Cedrus* abundance. The ~1000 cyclicity transitioned towards frequencies of ~1600 and ~2000 years in the Middle and Late Holocene between 6000–7000 cal yr BP in Sierra Nevada (Fig. 7B). A ~1000 yr frequency cycle also characterizes the Early and early-Middle Holocene of the Morocco *Cedrus* synthetic record which, similar to Sierra Nevada, appears to be muted since 6000 cal yr BP (Fig. 7E). The ~1000 yr cyclicity is one of the most pervasive cycles forced by solar activity, previously documented from the Mediterranean and North Atlantic (e.g., Debret et al., 2007, 2009; Fletcher et al., 2013; Ramos-Román et al., 2018a). The ~2000-year periodicity has also been described in paleoclimatic records from the study area as most-likely related with a solar origin or marine circulation (Rodrigo-Gámiz et al., 2014b; Ramos-Román et al., 2018a). We suggest that solar activity variations forced climate and vegetation changes in the Early Holocene, including forest oscillations and *Cedrus* pollen. A cyclicity of ~1600-1500 years has also been identified in other records from both the North Atlantic and western Mediterranean, including Morocco and the Sierra Nevada, and has been interpreted as both a solar and atmospheric-oceanic forcing mechanism (e.g. Bond et al., 2001; Rodrigo-Gámiz et al., 2014b; Jiménez-Espejo et al., 2014; García-Alix et al., 2017; Ramos-Román et al., 2018a). A transition in dominant periodicity of vegetation change from ~900 to 1000 to ~1750-2000 years in the Middle Holocene ~6000 cal yr BP was previously observed by Fletcher et al. (2013) and later by Ramos-Román et al. (2018a). Therefore, our data confirm previous studies that show the shift in periodicities from a climate system mostly controlled by external solar forcing during the Early and early-Middle Holocene that evolved to a system dominated by internal atmospheric-oceanic dynamics variability during the late-Middle and Late Holocene (Debret et al., 2009; Fletcher et al., 2013).

4.3. African climate, vegetation, dust flux and wind intensity

This study shows that the *Cedrus* pollen in European records can be mostly explained by the abundance of *Cedrus* in N Africa and its evolution throughout the Holocene depending on climate change. Therefore, the hypothesis of *Cedrus* occurrences in European records related with enhanced eolian activity during especially arid periods such as during the 8.2 and 4.2 ka events (Magri and Parra, 2002) needs modification. Those two periods were also arid in N Africa (Tierney et al., 2017), but in addition were cold, which would have had a positive impact in *Cedrus* populations, counterbalancing dryness by less evaporation-evapotranspiration in the mountain areas. An apparent contradiction also exists between precipitation records from this area, reflecting overall humid conditions during the Early and early-Middle Holocene – the African Humid Period (de Menocal et al., 2000; Tierney et al., 2017) – and overall low *Cedrus* abundances in N Africa (notice the negative correlations between *Cedrus* from Morocco and Sierra Nevada and precipitation in Table 3; Fig. 6). Even though it might have rained more, especially during winter (Zielhofer et al., 2019), the high summer insolation during the Early Holocene most-likely produced very high seasonality, summer drought and low representation of cool and hygrophilous and drought sensitive conifers such as *Cedrus*. On the other hand, other summer drought adapted forest species such as *Quercus* thrived in the study area during the Early and early-Middle Holocene (Ramos-Román et al., 2018a; Campbell et al., 2017; Zielhofer et al., 2019).

The dust records from NW Africa and Sierra Nevada covary ($r = 0.96$; $p < 0.01$; Table 3) and are strongly related to climate and vegetation evolution in the western Mediterranean and N Africa (deMenocal et al., 2000; Jiménez-Espejo et al., 2014; Mesa-Fernández et al., 2018). The comparison between the dust record from NW Africa and Sierra Nevada with the precipitation record from NW Africa shows strong negative correlations ($r \geq -0.7$; $p < 0.01$; Table 3). This indicates that they could be strongly related in a cause-effect relationship: high precipitation in the study area during the Early Holocene and early-Middle Holocene generated forested vegetation, which in turn caused low atmospheric dust production and transport to Europe (e.g., Sierra Nevada). The reduction in summer insolation during the Middle Holocene produced a change in seasonality and lower winter precipitation, generating aridification in the western Mediterranean area (Jiménez-Moreno and Anderson, 2012; Jiménez-Espejo et al., 2014; Jiménez-Moreno et al., 2015; Carrión et al., 2018). This climatic shift also marks the end of the African Humid Period in North Africa (at ~5500 cal yr BP; deMenocal et al., 2000) and related end of sapropel (S1) sedimentation in the Mediterranean (at ~6000 cal yr BP; Filippidi and De Lange, 2019) but the beginning of the enhancement of *Cedrus* abundance in mountain areas in N Morocco at about the same time (~6000 cal yr BP; Fig. 6). Therefore, *Cedrus* and dust records from N Africa and Sierra Nevada are closely related (see positive correlations in Table 3) because they depended on the same climatic control (i.e., insolation), but they were most likely independent of wind intensity. This is supported at shorter timescales by the fact that higher eolian input into the Sierra Nevada area and Algerian-Balearic basin during the DA and MCA, which was interpreted as indicating drier conditions and more persistent northwest African winds (Nieto-Moreno et al., 2011; Jiménez-Espejo et al., 2014; Mesa-Fernández et al., 2018), does not coincide with a higher input of wind-blown *Cedrus* in the pollen records from the Sierra Nevada or Alboran Sea, indicating that the *Cedrus* record from the Sierra Nevada reflects *Cedrus* abundance in N Morocco and not the strength or persistence of eolian input in this area. On the other hand, the Saharan dust Zr/Th record from Sierra Nevada and Zr/Al records from Algerian-Balearic basin show a decrease in eolian input during the LIA, contrary to the wind-blown *Cedrus* increase at that time.

4.4. Cedrus and wind direction

The Sierra Nevada *Cedrus* stack is more similar to the Middle Atlas records than to the Rif Mountains record from Bab El Karn (see correlations in Table 2). At present, *Cedrus* mostly occurs in the Middle Atlas (80% of its distribution area; Linares et al., 2011; Cheddadi et al., 2017, Fig. 1). This might have been true for the past and that is probably the reason why the *Cedrus* record from Sierra Nevada is more similar to the records from the Middle Atlas. *Cedrus* pollen data from Bab El Karn are negatively correlated with other pollen records from the Moroccan area (especially with the Tigalmamine and Ras El Ma) or show no correlation (Table 2). However, Bab el Karn and ODP 976 site *Cedrus* records are positively correlated ($r = 0.45$; $p < 0.01$). This shows that most of the pollen preserved in marine ODP site 976 has a Rif source, which makes sense, for ODP site 976 is closer to the Rif than for example MD95-2043 or Sierra Nevada. Alboran Sea surface marine circulation, characterized by two differentiated gyres in the western (Western Anticyclonic Gyre, WAG) and eastern (Western Anticyclonic Gyre;

EAG) areas (Ausín et al., 2015, Fig. 1A), probably precluded surface marine transport of pollen from the west to the east. In addition, these gyres can funnel the surface waters and particles from the edge to the center of the gyre, where the gyre is less dynamic and the pollen can flocculate and sink easily (Fabrés et al., 2002), palynologically isolating these two marine geographic areas. This also supports the differences among these two marine *Cedrus* records.

These dissimilarities in the windblown *Cedrus* pollen records could also be explained by the SW component of the prevailing wind direction coming from the South in the Alboran Sea and S Iberian Peninsula (Figs. 1 and 2). Cluster-mean backward wind trajectories for the last 50 years at the Sierra Nevada study sites support this statement and show an important wind component from the SSW passing throughout the Middle Atlas region during September and October, the months when *Cedrus* pollen is produced (Fig. 2). ODP 976 site would then be more influenced by windblown pollen originating from the Rif, more directly located to the SW than the Middle Atlas. Our data suggest that a similar seasonal SSW wind pattern could have been active in the western Mediterranean during the Holocene.

4.5. Human impact and Cedrus

Although previous studies show that forests dynamics in the western Mediterranean were mostly shaped by climate, human impact could have also altered the landscapes by logging, grazing, burning, mining and cultivation (Carrión et al., 2010). Humans have severely impacted the landscapes in the Mediterranean region in the last millennia, and significantly since the Bronze age (Sadori et al., 2011, 2013). *Cedrus* forest dynamics in Northern Africa could have also been driven by human activities (Cheddadi et al., 2017). The previously mentioned differences in the *Cedrus* records between the Middle Atlas and Rif Mountains during the Middle and Late Holocene (Fig. 4), with the decrease in *Cedrus* since 6000 cal yr BP in the Rifian region, could be partly explained by a higher human impact and exploitation of *Cedrus* in that region, in particular in the last ~3000 cal yr BP. In this respect, a series of Phoenician colonies were stablished along the Western Mediterranean coast during the 8th century BCE (~2800 cal yr BP) (Pappa, 2009; Guirguis, 2019), including the foundation of the Russadir city (Melilla, Spain) in the Rifian coast (López Pardo, 2015), when an important *Cedrus* pollen decline occurred (Fig. 4). It is well known that the Phoenicians preferentially favored cedar timber for ship construction, being a subject for profitable trade (Sommer, 2007). Phoenicians provided cedar timber to different kingdoms across the entire Mediterranean, such as Egyptians, who used it for ship construction, and for building palaces and religious sites (Manning et al., 2014; Liphschitz and Gideon, 1995) and for carpentry (Giachi et al., 2016). This prominent role of Phoenicians as timber providers was even recognized in the Bible "*As you know, we have no one as skilled in felling trees as the Sidonians*" (1 Kings 5:20). Western Mediterranean Phoenician shipwrecks in the Iberian margin also contain cedar timber as structural element (Negueruela, 2004). In any case, cedar was highly valued by shipwrights and other artisans for its water, rot and parasite resistance (Pulak, 2001) and recent studies indicate that cedar timber was obtained in many forests along the Mediterranean, and not exclusively in *Cedrus* forests located in Lebanon (Rich et al., 2016). The Rifian coastal area was highly populated during the Roman period compared with the more southern Middle Atlas region, which was a troublesome region and not included in the Roman empire (Whittaker, 1994). Therefore, a higher human pressure on the *Cedrus* forest in the Rifian coastal region in the past is expected, compared with more inland areas such as the Middle Atlas Mountains.

Human influence on the environments in the study area enhanced since 2000–1500 cal yr BP (Nour el Bait et al., 2014; Cheddadi et al., 2014; Campbell et al., 2017; Ramos-Román et al., 2018b). A significant decrease in *Cedrus* observed in both the Morocco and Sierra Nevada records at around 1400-1300 cal yr BP, during the DA and MCA periods could be due to the combination of extreme drought (see references above) and to the intensification of human activity at that time (Campbell et al., 2017). However, it is interesting to note that *Cedrus* increased again later on during the LIA, still under high or even higher anthropic pressure, which indicates that climate forcing was probably more important controlling forest dynamics at long- and short-time scales in north African mountain areas.

5. Conclusions

The synthesis and comparison of the Holocene *Cedrus* pollen records from Sierra Nevada in southern Spain, Alboran Sea and Morocco indicate that:

1. Significant similarities are observed between *Cedrus* pollen records in the study area, which show similar trends at long- and short-term time-scales. Therefore, windblown *Cedrus* pollen records from Sierra Nevada and southern Europe can be used as a proxy for environmental and climate change in northern Africa, if analyzed carefully.
2. *Cedrus* pollen abundances are generally low during the Early Holocene, increasing in the Middle and Late Holocene since ~6000 cal yr BP. This long-term trend is mostly related with changes in summer insolation, producing a decrease in mean annual temperatures and summer evaporation and evapotranspiration triggering the expansion of this cool-adapted and hygrophilous summer drought-sensitive species in the late-Middle and Late Holocene.
3. A significant *Cedrus* decrease occurred between 2000 and 600 cal yr BP during the DA and MCA periods most likely caused by enhanced persistent aridity/drought conditions. Anthropogenic activities could have also intensified *Cedrus* deforestation observed in the study area at that time. However, *Cedrus* populations seem to recover during the LIA. Colder and more humid conditions at that time would have benefited *Cedrus* growth and re-expansion in the Moroccan area.
4. Millennial-scale variability is also observed in the *Cedrus* abundances superimposed on the Holocene long-term trends. *Cedrus* records from the western Mediterranean show synchronous expansions at ~10,200, 9,000, 8200–7,800, 6900-6800, 6200–5,800, 4400–4,200, 2300 and 500-200 cal yr BP that generally occurred during well-known cold (e.g., ~8.2 and 4.2 ka events, LIA) and/or humid (e.g., IRHP, LIA), events in the western Mediterranean or North Atlantic areas, triggering *Cedrus* expansion in Morocco. This study also shows a change in the *Cedrus* abundance cyclical periodicities at ~6000 cal yr BP, from a 1000- to a 1600–2000-yr dominated cycles. This study confirms that this change in periodicities in the Middle Holocene seems to be a common feature in vegetation and paleoclimate records in the western Mediterranean and North Atlantic regions. This periodicity change was related with the establishment of the actual climate system in the western Mediterranean region, from being mostly controlled by external solar forcing to being dominated by internal atmospheric-oceanic dynamics.
5. The amount of *Cedrus* pollen that is transported to southern Europe seems to be mostly controlled by its abundance in northern Africa and not so much by wind intensity. Differences in windblown *Cedrus* records in southern Europe could be

explained by geographic distribution of *Cedrus* under a prevalent SW wind direction.

6. This study shows that *Cedrus* has been very sensitive to summer drought in the past. Predicted severe drought conditions for the next decades in northern Africa (IPCC, 2013) will greatly affect the already decreasing *Cedrus* populations.
7. Finally, our study shows that long distance and low concentration fossil pollen are useful in reconstructing paleoenvironments and paleoclimates when a good density of records is available for a certain geographic area.

Author statement

Gonzalo Jiménez-Moreno: Conceptualization, Methodology, Investigation, Writing −Original Draft, Visualization. R. Scott Anderson: Investigation, Writing- Review & Editing. María J. Ramos-Román: Investigation, Writing- Review & Editing. Jon Camuera: Investigation, Writing- Review & Editing. Jose Manuel Mesa-Fernández: Investigation, Writing- Review & Editing. Antonio García-Alix: Investigation, Writing - review & editing, Visualization. Francisco J. Jiménez-Espejo: Investigation, Writing - review & editing. José S. Carrion: Investigation, Writing - review & editing. Alejandro López-Avilés: Investigation, Visualization.

Declaration of competing interest

The authors declare that they have no known competing financial interests or personal relationships that could have appeared to influence the work reported in this paper.

Acknowledgements

Support for this study comes from projects CGL2013-47038-R and CGL2017-85415-R funded by Ministerio de Economía y Competitividad of Spain and Fondo Europeo de Desarrollo Regional FEDER; Séneca Project 20788/PI/18; Junta de Andalucía FEDER Project B-RNM-144-UGR18, UGR-FEDER B-RNM-144-UGR18 Proyectos I + D + i del Programa Operativo FEDER 2018 and the research group RNM-190 (Junta de Andalucía). M.J.R.R. acknowledges the postdoctoral funding provided by the European Commission/H2020 (ERC-2017-ADG, project number 788616). J.C. acknowledges the postdoctoral funding provided by the Academy of Finland (project number 316702). A.G.-A. acknowledges the Ramón y Cajal fellowship RYC-2015-18966 provided by the Ministerio de Economía y Competitividad of the Spanish Government. This paper greatly benefited from the reviews of two anonymous reviewers and from the editor Giovanni Zanchetta. Thanks to Rachid Cheddadi, William Fletcher and Nathalie Combourieu-Nebout for kindly providing pollen data from the Alboran Sea and N Morocco records.

References

Agencia Estatal de Meteorología AEMET, 2020. Online. http://www.aemet.es/es/serviciosclimaticos/datosclimatologicos. (Accessed 1 March 2020).

Abel-Schaad, D., Iriarte, E., López-Sáez, J.A., Pérez-Díaz, S., Sabariego Ruiz, S., Cheddadi, R., Alba-Sánchez, F., 2018. Are *Cedrus atlantica* forests in the Rif Mountains of Morocco heading towards local extinction? Holocene 28 (6), 1023–1037.

Alba-Sánchez, F., Abel-Schaad, D., López-Sáez, J.A., Sabariego Ruiz, S., Pérez-Díaz, S., González-Hernández, A., 2018. Paleobiogeografía de *Abies* spp. y *Cedrus atlantica* en el Mediterráneo Occidental (península ibérica y Marruecos). Ecosistemas 27 (1), 26–37.

Anderson, R.S., Jiménez-Moreno, G., Carrión, J.S., Pérez-Martínez, C., 2011. Holocene vegetation history from Laguna de Río Seco, Sierra Nevada, southern Spain. Quat. Sci. Rev. 30, 1615–1629.

Ausín, B., Flores, J.-., Sierro, F.J., Bárcena, M.A., Hernández-Almeida, I., Francés, G., Gutiérrez-Arnillas, E., Martrat, B., Grimalt, J.O., Cacho, I., 2015. Coccolithophore productivity and surface water dynamics in the Alboran Sea during the last 25kyr. Palaeogeogr., Palaeoclimatol. Palaeoecol 418, 126–140.

Bell, B.A., Fletcher, W.J., 2016. Modern surface pollen assemblages from the Middle and High Atlas, Morocco: insights into pollen representation and transport. Grana 55 (4), 286–301.

Bell, B., Fletcher, W.J., Cornelissen, H.L., Campbell, J.F.E., Ryan, P., Grant, H., Zielhofer, C., 2019. Stable carbon isotope analysis on fossil *Cedrus* pollen shows summer aridification in Morocco during the last 5000 years. J. Quat. Sci. 34 (4–5), 323–332.

Bini, M., Zanchetta, G., Perşoiu, A., Cartier, R., Català, A., Cacho, I., Dean, J.R., Di Rita, F., Drysdale, R.N., Finnè, M., Isola, I., Jalali, B., Lirer, F., Magri, D., Masi, A., Marks, L., Mercuri, A.M., Peyron, O., Sadori, L., Sicre, M.-A., Welc, F., Zielhofer, C., Brisset, E., 2019. The 4.2 ka BP Event in the Mediterranean region: an overview. Clim. Past 15, 555–577.

Bond, G., Kromer, B., Beer, J., Muscheler, R., Evans, M.N., Showers, W., Hoffmann, S., Lotti-Bond, R., Hajdas, I., Bonani, G., 2001. Persistent solar influence on North Atlantic climate during the Holocene. Science 294, 2130–2136.

Cacho, I., Grimalt, J.O., Pelejero, C., Canals, M., Sierro, F.J., Flores, J.A., Shackleton, N., 1999. Dansgaard-oeschger and heinrich event imprints in Alboran Sea paleotemperatures. Paleoceanography 14, 698–705.

Campbell, J.F.E., Fletcher, W.J., Joannin, S., Hughes, P.D., Rhanem, M., Zielhofer, C., 2017. Environmental drivers of Holocene forest development in the Middle Atlas, Morocco. Front. Ecol. Evol. 5, 113.

Camuera, J., Jiménez-Moreno, G., Ramos-Román, M.J., García-Alix, A., Toney, J.L., Anderson, R.S., Jiménez-Espejo, F., Bright, J., Webster, C., Yanes, Y., Carrión, J.S., 2019. Vegetation and climate changes during the last two glacial-interglacial cycles in the western Mediterranean: a new long pollen record from Padul (southern Iberian Peninsula). Quat. Sci. Rev. 205, 86–105.

Camuera, J., Jiménez-Moreno, G., Ramos-Román, M.J., García-Alix, A., Toney, J.L., Anderson, R.S., Jiménez-Espejo, F.J., Kaufman, D., Bright, J., Webster, C., Yanes, Y., Carrión, J.S., Ohkouchi, N., Suga, H., Yamame, M., Yokoyama, Y., Martínez-Ruiz, F., 2018. Orbital-scale environmental and climatic changes recorded in a new ~ 200,000-year-long multiproxy sedimentary record from Padul, southern Iberian Peninsula. Quat. Sci. Rev. 198, 91–114.

Carrión, J.S., Fierro, E., Ros, M., Munuera, M., Fernández, S., Ochando, J., Amorós, G., Navarro, F., Manzano, S., González-Sampériz, P., Moreno, A., 2018. Ancient forests in European drylands: Holocene palaeoecological record of Mazarrón, south-eastern Spain. P. Geologist Assoc, 4, 512–525.

Carrión, J.S., Sánchez-Gómez, P., Mota, J.F., Yll, R., Chaín, C., 2003. Holocene vegetation dynamics, fire and grazing in the Sierra de Gádor, southern Spain. Holocene 13, 839–849.

Carrión, J.S., Fuentes, N., González-Sampériz, P., Sánchez Quitante, L., Finlayson, J.C., Fernández, S., Andrade, A., 2007. Holocene environmental change in a montane region of southern Europe with a long history of human settlement. Quat. Sci. Rev. 26, 1455–1475.

Carrión, J.S., Fernández, S., González-Sampériz, P., Gil-Romera, G., Badal, E., Carrión-Marco, Y., López-Merino, L., López-Sáez, J.A., Fierro, E., Burjachs, F., 2010. Expected trends and surprises in the lateglacial and Holocene vegetation history of the iberian Peninsula and balearic islands. Rev. Palaeobot. Palynol. 162 (3), 458–475.

Català, A., Cacho, I., Frigola, J., Pena, L.D., Lirer, F., 2019. Holocene hydrography evolution in the Alboran Sea: a multi-record and multi-proxy comparison. Clim. Past 15, 927–942.

Cheddadi, R., Lamb, H.F., Guiot, J., van der Kaars, S., 1998. Holocene climatic change in Morocco: a quantitative reconstruction from pollen data. Clim. Dynam. 14, 883–890.

Cheddadi, R.B., Fady, L., François, L., Hajar, J.-P., Suc, K., Huang, K., Demarteau, M., Vendramin, G.G., Ortu, E., 2009. Putative glacial refugia of *Cedrus atlantica* deduced from quaternary pollen records and modern genetic diversity. J. Biogeogr. 36, 1361–1371.

Cheddadi, R., Bouaissa, O., Rhoujjati, A., Dezileau, L., 2016. Environmental changes in the moroccan western Rif Mountains over the last 9,000 years. Quaternaire 27, 15–25.

Cheddadi, R., Henrot, A.-J., François, L., Boyer, F., Bush, M., Carré, M., Coissac, E., De Oliveira, P.E., Ficetola, F., Hambuckers, A., Huang, K., Lézine, A.-M., Nourelbait, M., Rhoujjati, A., Taberlet, P., Sarmiento, F., Abel-Schaad, D., Alba-Sánchez, F., Zheng, Z., 2017. Microrefugia, climate change, and conservation of *Cedrus atlantica* in the Rif mountains, Morocco. Front. Ecol. Evol. 5, 114.

Combourieu-Nebout, N., 1993. Vegetation response to upper Pliocene glacial/interglacial cyclicity in the central Mediterranean. Quat. Res. 4, 228–236.

Combourieu Nebout, N., Peyron, O., Dormoy, I., Desprat, S., Beaudouin, C., Kotthoff, U., Marret, F., 2009. Rapid climatic variability in the west Mediterranean during the last 25 000 years from high resolution pollen data. Clim. Past 5, 503–521.

Copes-Gerbitz, K., Fletcher, W., Lageard, J.G., Rhanem, M., Harrison, S.P., 2019. Multidecadal variability in Atlas cedar growth in Northwest Africa during the last 850 years: implications for dieback and conservation of an endangered species. Dendrochronologia 56, 125599.

Debret, M., Bout-Roumazeilles, V., Grousset, F., Desmet, M., McManus, J.F., Massei, N., Sebag, D., Petit, J.-R., Copard, Y., Trentesaux, A., 2007. The origin of the 1500-year climate cycles in Holocene North-Atlantic records. Clim. Past 3, 569–575.

Debret, M., Sebag, D., Crosta, X., Massei, N., Petit, J.-R., Chapron, E., Bout-Roumazeilles, V., 2009. Evidence from wavelet analysis for a mid-Holocene

transition in global climate forcing. Quat. Sci. Rev. 28, 2675–2688.
deMenocal, P., Ortiz, J., Guilderson, T., Sarnthein, M., 2000. Coherent high- and low-latitude climate variability during the Holocene warm period. Science 288, 2198–2202.
Di Rita, F., Magri, D., 2019. The 4.2 ka event in the vegetation record of the central Mediterranean. Clim. Past 15, 237–251.
Dormoy, I., Peyron, O., Combourieu Nebout, N., Goring, S., Kotthoff, U., Magny, M., Pross, J., 2009. Terrestrial climate variability and seasonality changes in the Mediterranean region between 15 000 and 4000 years BP deduced from marine pollen records. Clim. Past 5, 615–632.
Esper, J., Frank, D., Büntgen, U., Verstege, A., Luterbacher, J., Xoplaki, E., 2007. Long-term drought severity variations in Morocco. Geophys. Res. Lett. 34, L17702.
Fabrés, J., Calafat, A., Sanchez-Vidal, A., Canals, M., Heussner, S., 2002. Composition and spatio-temporal variability of particle fluxes in the western alboran gyre, Mediterranean sea. J. Marine Syst 33, 431–456.
Filippidi, A., De Lange, G.J., 2019. Eastern Mediterranean deep water formation during sapropel S1: a reconstruction using geochemical records along a bathymetric transect in the Adriatic outflow region. Paleoceanogr. Paleoclimatol 34, 409–429.
Fletcher, W.J., Sanchez Goñi, M.F., 2008. Orbital and sub-orbital scale climate impacts on the vegetation of the W. Mediterranean basin during the last 48 000 years. Quat. Res. 70, 451–464.
Fletcher, W.J., Debret, M., Goñi, M.F.S., 2013. Mid-Holocene emergence of a low-frequency millennial oscillation in western Mediterranean climate: implications for past dynamics of the North Atlantic atmospheric westerlies. Holocene 23 (2), 153–166.
Frisia, S.A., Borsato, A., Mangini, A., Spötl, C., Madonia, G., Sauro, U., 2006. Holocene climate variability from a discontinuous stalagmite record and the Mesolithic to Neolithic transition. Quat. Res. 66, 388–400.
García-Alix, A., Jiménez-Espejo, F.J., Toney, J.L., Jiménez-Moreno, G., Ramos-Román, M.J., Anderson, R.S., Ruano, P., Queralt, I., Delgado Huertas, A., Kuroda, J., 2017. Alpine bogs of southern Spain show human-induced environmental change superimposed on long-term natural variations. Sci. Rep. 7, 7439.
García-Alix, A., Jiménez-Espejo, F.J., Jiménez-Moreno, G., Toney, J.L., Ramos-Román, M.J., Camuera, J., Anderson, R.S., Delgado Huertas, A., Martínez-Ruiz, Queralt, I., 2018. Holocene geochemical footprint from Semi-arid alpine wetlands in southern Spain. Sci. Data 5, 180024.
Gehrig-Fasel, J., Guisan, A., Zimmermann, N.E., 2008. Evaluating thermal treeline indicators based on air and soil temperature using an air-to-soil temperature transfer model. Ecol. Model. 213, 345–355.
Giachi, G., Guidotti, M.C., Lazzeri, S., Sozzi, L., Macchioni, N., 2016. Wood identification of the headrests from the collection of the Egyptian Museum in Florence. J. Archaeol. Sci.: For. Rep. 9, 340–346.
Gomes, S., Fletcher, W.J., Rodrigues, T., Stone, A., Abrantes, F., Naughton, F., 2020. Time-transgressive Holocene maximum of temperate and Mediterranean forest development across the Iberian Peninsula reflects orbital forcing. Palaeogeogr., Palaeoclimatol. Palaeoecol 550, 109739.
González-Sampériz, P., Leroy, S.A., Carrión, J.S., Fernández, S., García-Antón, M., Gil-García, M.J., et al., 2010. Steppes, savannahs, forests and phytodiversity reservoirs during the Pleistocene in the Iberian Peninsula. Rev. Palaeobot. Palynol. 162 (3), 427–457.
Guirguis, M., 2019. Central North Africa and Sardinian connections (end of 9th-8th century BC). The multi-ethnic and multicultural facies of the earliest western Phoenician Communities. Arid zone Archaeol. Monograph 8, 111–115.
Hammer, Ø., Harper, D.A.T., Ryan, P.D., 2001. PAST: Paleontological statistics software Package for education and data analysis. Palaeontol. Electron 4 (1), 9.
Holzwarth, U., Meggers, H., Esper, O., Kuhlmann, H., Freudenthal, T., Hensen, C., Zonneveld, K.A.F., 2010. NW African climate variations during the last 47,000 years: evidence from organic-walled dinoflagellate cysts. Palaeogeogr., Palaeoclimatol. Palaeoecol 291, 443–455.
IPCC, 2013. Summary for Policymakers. In: Stocker, T.F., Qin, D., Plattner, G.-K., Tignor, M., Allen, S.K., Boschung, J., Nauels, A., Xia, Y., Bex, V., Midgley, P.M. (Eds.), Climate Change 2013: the Physical Science Basis. Contribution of Working Group I to the Fifth Assessment Report of the Intergovernmental Panel on Climate Change. Cambridge University Press, Cambridge, United Kingdom and New York, NY, US.
Jalut, G., Dedoubat, J.J., Fontugne, M., Otto, T., 2009. Holocene circum-Mediterranean vegetation changes: climate forcing and human impact. Quat. Int. 200, 4–18.
Jiménez-Espejo, F.J., García-Alix, A., Jiménez-Moreno, G., Martínez-Ruiz, F., Anderson, R.S., Rodríguez-Tovar, F.J., Giralt, S., Rodrigo-Gámiz, M., Delgado Huertas, A., Pardo-Igúzquiza, E., 2014. Saharan aeolian input and effective humidity variations over Western Europe during the Holocene. Chem. Geol. 374–375, 1–12.
Jiménez-Moreno, G., Anderson, R.S., 2012. Holocene vegetation and climate change recorded in alpine bog sediments from the Borreguiles de la Virgen, Sierra Nevada, southern Spain. Quat. Res. 77, 44–53.
Jiménez-Moreno, G., García-Alix, A., Hernández-Corbalán, M.D., Anderson, R.S., Delgado-Huertas, A., 2013. Vegetation, fire, climate and human disturbance history in the southwestern Mediterranean area during the late Holocene. Quat. Res. 79, 110–122.
Jiménez-Moreno, G., Rodríguez-Ramírez, A., Pérez-Asensio, J.N., Carrión, J.S., López-Sáez, J.A., Villarías-Robles, J.J.R., Celestino-Pérez, S., Cerrillo-Cuenca, E., Ángel León, A., Contreras, C., 2015. Impact of late-Holocene aridification trend, climate variability and geodynamic control on the environment from a coastal area in SW Spain. Holocene 25, 607–617.
Lamb, H.F., van der Kaars, S., 1995. Vegetational response to Holocene climatic change: pollen and palaeolimnological data from the Middle Atlas, Morocco. Holocene 5, 400–408.
Lamb, H., Roberts, N., Leng, M., Barker, P., Benkaddour, A., van der Kaars, S., 1999. Lake evolution in a semi-arid montane environment: response to catchment change and hydroclimatic variation. J. Paleolimnol. 21, 325–343.
Laskar, J., Robutel, P., Joutel, F., Gastineau, M., Correia, A.C.M., Levrard, B., 2004. A long term numerical solution for the insolation quantities of the Earth. Astron. Astrophys. Nor. 428, 261–285.
Linares, J.C., Taïqui, L., Camarero, J.J., 2011. Increasing drought sensitivity and decline of Atlas cedar (*Cedrus atlantica*) in the Moroccan Middle Atlas forests. Forests 2, 777–796.
Lionello, P., Malanotte-Rizzoli, P., Boscolo, R., Alpert, P., Artale, V., Li, L., Luterbacher, J., May, W., Trigo, R., Tsimplis, M., Ulbric, U., Xoplaki, E., 2006. The Mediterranean climate: an overview of the main characteristics and issues. In: Lionello, P., Malanotte-Rizzoli, P., Boscolo, R. (Eds.), Mediterranean Climate Variability, Developments in Earth and Environmental Sciences, 4. Elsevier, Amsterdam, pp. 1–26.
Liphschitz, N., Biger, G., 1995. The timber trade in ancient Palestine. Tel Aviv 22 (1), 121–127.
López-Pardo, F., 2015. Russadir: from the literally Memory to the historical reality of the Phoenician-Punic expansion in west. Gerión 33, 91–103.
Magny, M., De Beaulieu, J.L., Drescher-Schneider, R., Vanniere, B., Walter-Simonnet, A.V., Miras, Y., Millet, L., Bossuet, G., Peyron, O., Brugiapaglia, E., Leroux, A., 2007. Holocene climate changes in the central Mediterranean as recorded by lake-level fluctuations at Lake Accesa (Tuscany, Italy). Quat. Sci. Rev. 26, 1736–1758.
Magri, D., 2012. Quaternary history of Cedrus in southern Europe. Ann. Bot. 2, 57–66.
Magri, D., Parra, I., 2002. Late Quaternary western Mediterranean pollen records and African winds. Earth Planet Sci. Lett. 200, 401–408.
Magri, D., Di Rita, F., Aranbarri, J., Fletcher, W., González-Sampériz, P., 2017. Quaternary disappearance of tree taxa from Southern Europe: timing and trends. Quat. Sci. Rev. 163, 23–55.
Malanson, G.P., Resler, L.M., Butler, D.R., Fagre, D.B., 2019. Mountain plant communities: uncertain sentinels? Prog. Phys. Geogr. 43, 521–543.
Manning, S.W., Dee, M.W., Wild, E.M., Bronk Ramsey, C., Bandy, K., Creasman, P.P., Griggs, C.B., Pearson, C.L., Shortland, A.J., Steier, P., 2014. High-precision dendro-14C dating of two cedar wood sequences from First Intermediate Period and Middle Kingdom Egypt and a small regional climate-related 14C divergence. J. Archaeol. Sci. 46, 401–416.
Manzano, S., Carrión, J.S., López-Merino, L., Jiménez-Moreno, G., Toney, J.L., Amstrong, H., Anderson, R.S., García-Alix, A., Pérez, J.L.G., Sánchez-Mata, D., 2019. A palaeoecological approach to understanding the past and present of Sierra Nevada, a Southwestern European biodiversity hotspot. Global Planet. Change 175, 238–250.
Martín-Puertas, C., Valero-Garcés, B.L., Brauer, A., Mata, M.P., Delgado-Huertas, A., Dulski, P., 2009. The iberian-roman Humid Period (2600–1600 cal yr BP) in the zoñar lake varve record (Andalucía, southern Spain),. Quat. Res. 71, 108–120.
Meijer, P.T., Tuenter, E., 2007. The effect of precession-induced changes in the Mediterranean freshwater budget on circulation at shallow and intermediate depth. J. Mar. Syst. 68, 349–365.
Mesa-Fernández, J.M., Jiménez-Moreno, G., Rodrigo-Gámiz, M., García-Alix, A., Jiménez-Espejo, F.J., Martínez-Ruiz, F., Anderson, R.S., Camuera, J., Ramos-Román, M.J., 2018. Vegetation and geochemical responses to Holocene rapid climate change in the Sierra Nevada (southeastern Iberia): the Laguna Hondera record. Clim. Past 14, 1687–1706.
Morales-Molino, C., García-Antón, M., Postigo-Mijarra, J.M., Morla, C., 2013. Holocene vegetation, fire and climate interactions on the westernmost fringe of the Mediterranean Basin. Quat. Sci. Rev. 59, 5–17.
Negueruela, I., 2004. Hacia la comprensión de la construcción naval fenicia según el barco «Mazarrón-2» del siglo VII a. C. In: Mederos, A., Peña, V., Wagner, C.G. (Eds.), La navegación fenicia: tecnología naval y derroteros: encuentro entre marinos, arqueólogos e historiadores. Centro de Estudios Fenicio-Púnicos, Madrid, pp. 227–278.
Nieto-Moreno, V., Martínez-Ruiz, F., Giralt, S., Jiménez-Espejo, F., Gallego-Torres, D., Rodrigo-Gámiz, M., García-Orellana, J., Ortega-Huertas, M., de Lange, G J, 2011. Tracking climate variability in the western Mediterranean during the Late Holocene: a multiproxy approach. Clim. Past 7, 1395–1414.
Nieto-Moreno, V., Martínez-Ruiz, F., Giralt, S., Gallego-Torres, D., García-Orellana, J., Masqué, P., Ortega-Huertas, M., 2013. Climate imprints during the 'medieval climate anomaly' and the 'little ice age' in marine records from the Alboran Sea basin. Holocene 23 (9), 1227–1237.
Nour El Bait, M., Rhoujjati, A., Eynaud, F., Benkaddour, A., Dezileau, L., Wainer, K., Goslar, T., Khater, C., Tabel, J., Cheddadi, R., 2014. An 18 000-year pollen and sedimentary record from the cedar forests of the Middle Atlas, Morocco. J. Quat. Sci. 29, 423–432.
Ojeda, F., Arroyo, J., Marañón, T., 1998. The phytogeography of European and Mediterranean heath species (Ericoideae, Ericaceae): a quantitative analysis. J. Biogeogr. 25 (1), 165–178.
Oliva, M., Ruiz-Fernández, J., Barriendos, M., Benito, G., Cuadrat, J.M., Domínguez-Castro, F., García-Ruiz, J.M., Giralt, S., Gómez-Ortiz, A., Hernández, A., López-Costas, O., López-Moreno, J.I., López-Sáez, J.A., Martínez-Cortizas, A., Moreno, A., Prohom, M., Saz, M.A., Serrano, E., Tejedor, E., Trigo, R., Valero-Garcés, B.,

Vicente-Serrano, S.M., 2018. The little ice age in iberian mountains,. Earth Sci. Rev. 177, 175–208.
Oliveira, D., Desprat, S., Rodrigues, T., Naughton, F., Hodell, D., Trigo, R., Rufino, M., Lopes, C., Abrantes, F., Sánchez Goñi, M.F., 2016. The complexity of millennial-scale variability in southwestern Europe during MIS 11. Quat. Res. 86 (3), 373–387.
Olmedo-Cobo, J.A., Cunill-Artigas, R., Martínez-Ibarra, E., Gómez-Zotano, J., 2017. Paleoecología de *Abies* sp. en Sierra Bermeja (sur de la Península Ibérica) durante el Holoceno medio a partir del análisis pedoantracológico. Bosque 38 (2), 259–270.
Paillard, D., Labeyrie, L., Yiou, P., 1996. Macintosh program performs time-series analysis. Eos Trans. AGU 77, 379.
Pappa, E., 2009. Reflections on the earliest Phoenician presence in north-west Africa. Talanta XL-XLI 53–72.
Pérez-Luque, A.J., Pérez-Pérez, R., Bonet, F.J., Zamora, R., 2012. Proyecto: Seguimiento de los efectos de cambio global en Sierra Nevada: diseño y desarrollo de un sistema de monitorización ecológica basado en la red de estaciones multiparamétricas. In: XI Congreso Nacional de Medio Ambiente.
Postigo-Mijarra, J.M., Morla, C., Barrón, E., Morales-Molino, C., García, S., 2010. Patterns of extinction and persistence of arctotertiary flora in Iberia during the quaternary. Rev. Palaeobot. Palynol. 162, 416–426.
Power, M.J., Marlon, J., Ortiz, N., et al., 2008. Changes in fire regimes since the Last Glacial Maximum: an assessment based on a global synthesis and analysis of charcoal data. Clim. Dynam. 30, 887–907.
Pulak, C., 2001. Cedar for ships. Archaeology and History in the Lebanon 14, 24–36.
Ramos-Román, M.J., Jiménez-Moreno, G., Anderson, R.S., García-Alix, A., Toney, J.L., Jiménez-Espejo, F.J., Carrión, J.S., 2016. Centennial-scale vegetation and north atlantic oscillation changes during the late Holocene in the western Mediterranean. Quat. Sci. Rev. 143, 84–95.
Ramos-Román, M.J., Jiménez-Moreno, G., Camuera, J., García-Alix, A., Anderson, R.S., Jiménez-Espejo, F.J., Sachse, D., Toney, J.L., Carrión, J.S., Webster, C., Yanes, Y., 2018a. Millennial-scale cyclical environment and climate variability during the Holocene in the western Mediterranean region deduced from a new multiproxy analysis from the Padul record (Sierra Nevada, Spain). Global Planet. Change 168, 35–53.
Ramos-Román, M.J., Jiménez-Moreno, G., Camuera, J., García-Alix, A., Anderson, R.S., Jiménez-Espejo, F.J., Carrión, J.S., 2018b. Holocene climate aridification trend and human impact interrupted by millennial- and centennial-scale climate fluctuations from a new sedimentary record from Padul (Sierra Nevada, southern Iberian Peninsula). Clim. Past 14, 117–137.
Rich, S., Manning, S.W., Degryse, P., Vanhaecke, F., Latruwe, K., van Lerberghe, K., 2016. To put a cedar ship in a bottle: dendroprovenancing three ancient East Mediterranean watercraft with the 87Sr/86Sr isotope ratio. J. Archaeol. Sci.: For. Rep. 9, 514–521.
Rodrigo-Gámiz, M., Martínez-Ruiz, F., Rampen, S.W., Schouten, S., Sinninghe Damsté, J.S., 2014. Sea surface temperature variations in the western Mediterranean Sea over the last 20 kyr: a dual-organic proxy ($U^{K'}_{37}$ and LDI) approach. Paleoceanography 29, 87–98.
Rodrigo-Gámiz, M., Martínez-Ruiz, F., Rodríguez-Tovar, F.J., Jiménez-Espejo, F.J., Pardo-Igúzquiza, E., 2014. Millennial- to centennial-scale climate periodicities and forcing mechanisms in the westernmost Mediterranean for the past 20,000 yr. Quat. Res. 81, 78–93.
Sadori, L., Jahns, S., Peyron, O., 2011. Mid-Holocene vegetation history of the central Mediterranean. Holocene 21, 117–129.
Sadori, L., Ortu, E., Peyron, O., Zanchetta, G., Vanniére, B., Desmet, M., Magny, M., 2013. The last 7 millennia of vegetation and climate changes at Lago di Pergusa (central Sicily, Italy). Clim. Past 9, 1969–1984.
Samartin, S., Heiri, O., Joos, F., Renssen, H., Franke, J., Brönnimann, S., Tinner, W., 2017. Warm Mediterranean mid-Holocene summers inferred from fossil midge assemblages. Nat. Geosci. 10, 207–212.
Sánchez, E., Gallardo, C., Gaertner, M.A., Arribas, A., Castro, M., 2004. Future climate extreme events in the Mediterranean simulated by a regional climate model: a first approach. Global Planet. Change 44, 163–180.
Schulz, M., Mudelsee, M., 2002. REDFIT: estimating red-noise spectra directly from unevenly spaced paleoclimatic time series. Comput. Geosci. 28, 421–426.
Sommer, M., 2007. Networks of commerce and knowledge in the Iron age: the case of the Phoenicians. Mediterr. Hist. Rev. 22 (1), 97–111.
Thuiller, W., Lavorel, S., Araujo, M.B., Sykes, M.T., Prentice, I.C., 2005. Climate change threats to plant diversity in Europe. Proc. Natl. Acad. Sci. Unit. States Am. 102, 8245–8250.
Toney, J.L., García-Alix, A., Jiménez-Moreno, G., Anderson, R.S., Moossen, H., Seki, O., 2020. New insights into Holocene hydrology and temperature from lipid biomarkers in western Mediterranean alpine wetlands. Quat. Sci. Rev. 240, 106395.
Trigo, R.M., Osborn, T.J., Corte-Real, J.M., 2002. The North Atlantic oscillation influence on Europe: climate impacts and associated physical mechanisms. Clim. Res. 20, 9–17.
Trigo, R.M., Pozo-Vázquez, D., Osborne, T., Castro-Díez, Y., Gómiz-Fortis, S., Esteban-Parra, M.J., 2004. North Atlantic oscillation influence on precipitation, river flow and water resources in the Iberian Peninsula. Int. J. Climatol. 24, 925–944.
Trouet, V., Esper, J., Graham, N.E., Baker, A., Scourse, J.D., Frank, D.C., 2009. Persistent positive North Atlantic oscillation mode dominated the medieval climate anomaly. Science 324, 78–80.
van der Hammen, T., Wijmstra, T.A., Zagwijn, H., 1971. The floral record of the late cenozoic of Europe. In: Turekian, K.K. (Ed.), The Late Cenozoic Glacial Ages. Yale University Press, New Haven, pp. 391–424.
Whittaker, C.R., 1994. Frontiers of the Roman Empire: a Social and Economic Study. Jhon Hopkins University press, Baltimore.
Zielhofer, C., Fletcher, W.J., Mischke, S., De Batist, M., Campbell, J.F.E., Joannin, S., Tjallingii, R., El Hamouti, N., Junginger, A., Stele, A., Bussmann, J., Schneider, B., Lauer, T., Spitzer, K., Strumpler, M., Brachert, T., Mikdad, A., 2017. Atlantic forcing of Western Mediterranean winter rain minima during the last 12,000 years. Quat. Sci. Rev. 157, 29–51.
Zielhofer, C., Köhler, A., Mischke, S., Benkaddour, A., Mikdad, A., Fletcher, W.J., 2019. Western Mediterranean hydro-climatic consequences of Holocene ice-rafted debris (Bond) events. Clim. Past 15, 463–475.